JOURNAL OF GEOPHYSICAL RESEARCH, VOL. 103, NO. A6, PAGES 11,725–11,744, JUNE 1, 1998

Satellite observations of lightning-induced electron precipitation

H. D. Voss,[1] M. Walt,[2] W. L. Imhof,[3] J. Mobilia,[3] and U. S. Inan[2]

Abstract. Lightning-induced electron precipitation (LEP) from the Earth's radiation belt has been observed on numerous occasions with detectors on the low-altitude S81-1/SEEP satellite. A sequence of seven LEP events on September 9, 1982, and eight events on October 20, 1982, are correlated on a one-to-one basis with one-hop whistlers at Palmer, Antarctica. The temporal profile within a LEP burst has a remarkable fine structure. It is shown to be associated with bunches of magnetically guided and focused 100-to-200 keV electrons that are repeatedly scattered by the atmosphere and bounce between the northern and southern hemispheres. The delay time between the lightning sferic and the arrival of the first electron bunch increases with increasing L as predicted by the first-order gyroresonance theory. The global distribution of strong LEP events observed with the SEEP payload correlates with lightning activity and shows a preferred distribution at $2 < L < 3$. This L shell range corresponds to the slot region in the electron radiation belt. A single LEP burst (10^{-3} erg s^{-1} cm^{-2}) in the slot region is estimated to deplete ~0.001% of the particles in the region covered by the burst magnetic field lines. The evidence supports the production of structured LEP by ducted rather than nonducted whistlers. It is found that ducted whistlers can be an important pitch angle diffusion mechanism for 100–250 keV electrons in the $2 < L < 3$ range although a number of uncertainties in the various parameters remain to be resolved. It is suggested that observations of LEP can be a new tool to measure the presence and transverse dimensions of plasmaspheric whistler mode ducts.

1. Introduction

Lightning-induced electron precipitation (LEP) from the Earth's radiation belts, caused by whistler wave-particle interactions, is a known troposphere-to-magnetosphere coupling mechanism. Experimental evidence for these phenomena includes ELF, VLF, and MF wave propagation anomalies or Trimpi events [*Helliwell et al.*, 1973; *Carpenter et al.*, 1984; *Burgess and Inan*, 1993]; balloon measurements [*Rosenberg et al.*, 1971]; rocket measurements [*Rycroft*, 1973; *Goldberg et al.*, 1987]; and satellite measurements [*Voss et al.*, 1984; *Imhof et al.*, 1986]. Electron-cyclotron (whistler) waves, which are believed to scatter the electrons, are electromagnetic plasma waves which propagate with right-circular polarization in field-aligned ducts of enhanced ionization. Pitch angle scattering of energetic radiation belt electrons by whistler mode waves can result in the precipitation of these electrons into the atmosphere [*Dungey*, 1963; *Cornwall*, 1964; *Roberts*, 1969; *Inan et al.*, 1978; and *Chang and Inan*, 1985]. While the evidence for such direct precipitation is now overwhelming and the causes of Trimpi events are well understood, the significance of this effect for major geophysical processes, such as trapped electron loss rates and ionospheric perturbations, is not clear. Additional data on the LEP effect are needed both to clarify the physical processes involved and to evaluate the impact of these sporadic precipitation events on the magnetosphere and ionosphere.

Electron spectroscopy measurements from a low-altitude (~220 km) satellite at L ~2.2 have on occasion shown a one-to-one correlation of precipitation bursts with ducted whistlers [*Voss et al.*, 1984; *Imhof et al.*, 1986]. These measurements were obtained with the Stimulated Emissions of Energetic Particles (SEEP) experiment on the three-axis stabilized, low-altitude (170–280 km), polar orbiting S81-1 satellite. The mission operation time for this satellite was May 1982 to December 1982. The satellite location relative to the radiation belt and the wave-particle interaction region is schematically illustrated in Figure 1. In this figure lightning flashes in the northern hemisphere produce whistlers which propagate along field lines toward the southern hemisphere, deflecting some of the north-bound electrons into trajectories which carry them to the S81-1 satellite. Because the SEEP particle detectors had relatively large geometric factors and the satellite was below the interfering background of trapped radiation for much of its orbit, the SEEP sensors had a high signal-to-background ratio for measuring low intensity fluxes of electrons in the bounce and drift loss cones. During most of the satellite lifetime, VLF wave data were recorded at ground stations in Antarctica for comparison with the precipitating particle events.

The emphasis of this paper is on the experimental measurements made with the SEEP detectors over a 6-month period in which numerous cases of LEP were observed. A previous brief report [*Voss et al.*, 1984] describes several cases of LEP detected on September 9, 1982, and a detailed simulation of the whistler wave-electron interaction was completed for one event [*Inan et al.*, 1989]. Other examples of LEP were described briefly in studies of short-duration electron precipitation bursts [*Imhof et al.*, 1986, 1989]. However, during the life of S81-1 over 100 events with electron signatures identical to

[1]Department of Physics, Taylor University, Upland, Indiana.
[2]STAR Laboratory, Stanford University, Stanford, California.
[3]Lockheed Martin Advanced Technology Center, Palo Alto, California.

Paper number 97JA02878.
0148-0227/98/97JA-02878$09.00

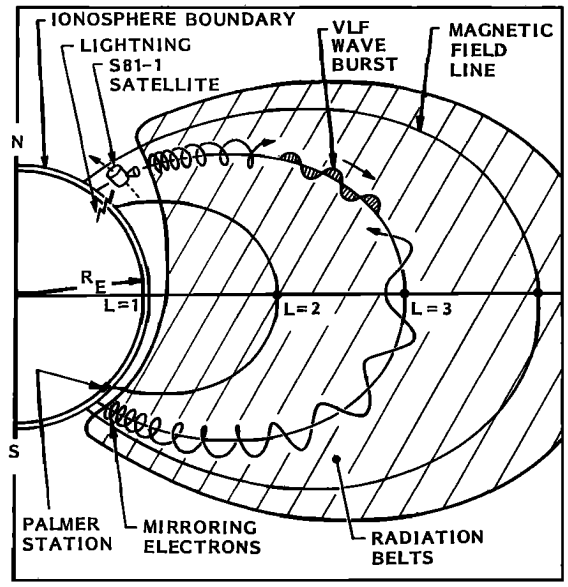

Figure 1. Schematic view of the satellite-radiation belt geometry for detecting lightning-induced electron precipitation.

those of the previously reported LEP were recorded. This unique data set allows a more complete study of the LEP process and an assessment of its overall global significance. These data also contain information bearing on the presence and sizes of plasmaspheric ducts which appear to guide the whistler waves responsible for LEP. Our primary purposes in this paper are to report on the energy and time structure of several lightning-induced electron precipitation bursts, show the global distribution of LEP bursts, estimate the induced loss rate of electrons from the radiation belt, and infer the characteristics of magnetospheric ducts from the LEP signatures. The possibility of using satellite traces of LEP to assess the transverse dimensions of plasmaspheric ducts has not been considered previously.

The detailed spectroscopic measurements of lightning-induced electron precipitation bursts afford a powerful technique to (1) clarify the complex physics of the wave-particle interaction, (2) evaluate the magnitude of radiation belt loss processes associated with terrestrial lightning, (3) study the atmospheric scattering and energy loss processes for electrons near the edge of the loss cone, (4) determine the spatial and temporal conductivity enhancements in the lower ionosphere produced by LEP events (associated with Trimpi events), (5) investigate the modes of wave propagation in the magnetosphere that are conducive to LEP electron precipitation, and (6) identify the magnetospheric duct structures which guide VLF waves.

2. Instrumentation

The SEEP payload included a cooled, solid-state particle spectrometer array with eight detectors. These detectors had large geometric factors, high energy resolution and covered the energy range 2-to-1000 keV for electrons and 10-to-1500 keV for protons [*Voss et al.*, 1982a]. The total equipment package also contained optical photometers, a plasma probe, and an X ray imaging spectrometer. We describe here, briefly, the distinctive features of each detector and present for completeness a full summary of the SEEP instrumentation in Table 1.

The main results presented in this paper were obtained from the electron detectors designated LE5, TE2, and ME1. The trapped energetic electron spectrometer TE2 (with a 20° conical half-angle field of view) was aligned perpendicularly to the orbit plane to measure electrons with pitch angles near 90°. It was cooled to −120°C to achieve a system noise resolution of 1.3 keV full width at half maximum (FWHM). A similar detector, LE5, was positioned 50° from the zenith. The medium energy, ME1, precipitating electron spectrometer (30° conical half-angle field of view) was aligned in the zenith direction and

Table 1. SEEP Instrumentation

Detector	Measurement	Range, keV	Energy Channels	Energy Resolution, keV FWHM	Temporal Resolution, s	Det Area, cm^2	Field of View, deg	Geometrical Factor, cm^2 sr	Pointing From Zenith
LE1	electrons	10–200	16–256	4	0.128	1.5	±20	0.17	10°
	protons	30–200							
LE2	electrons	6–200	16–256	2.1	0.128	0.5	±20	0.17	50°
	protons	10–200							
TE1	electrons	3–180	16–256	1.3	0.128	0.5	±20	0.17	90°
	protons	30–180							
LE4	electrons	magnet	16–256	4	0.128	0.5	±6	0.1	50°
	protons	20–200							
LE5	electrons	2–200	16–256	1	0.128	0.5	±20	0.17	50°
	protons	30–200							
TE2	electrons	6–950	256	1.3	0.063	0.5	±20	0.17	90°
	protons	30–950							
ME1	electrons	45–1000	256	14	0.063	2.94	±30	2.47	0°
	protons	450–1500							
ME2	electrons	45–1000	256	20	0.063	2.94	±30	2.47	180°
	protons	450–1500							
AP	photometer	391.4 nm	1	0.8 nm	0.245	3.0	±4	...	125°
		391.4 nm	1	2.4 nm					
		630.0 nm	1	1.2 nm					
PPM	plasma	10^2–10^5 cm^{-3}	...	...	0.063	2.0	...	...	35°
XRIS	X rays	4–40	24	21%	0.031	590	±90	6.0	125°

TE1 and TE2 have a common sensor but use different processing electronics.

had a 14 keV FWHM resolution. Since few electrons were expected from the zenith direction, the geometric factor of ME1 was large (2.47 cm^2 sr). The particle pitch angles observed at any time by these detectors depend on the inclination and declination of the magnetic field at the satellite location. However, in general, TE2 viewed electrons near 90°, ME1 observed electrons at small pitch angles (<30°) and LE5 was oriented between these values. TE2 and LE5 are sensitive to both electrons and ions. LE4 used a sweeping magnet to reject electrons below 1 MeV to give a measurement of ion fluxes. In the LEP events described in this paper the ion fluxes were negligible.

Two pulse height analysis techniques were used for the SEEP particle spectrometers. The LE1, LE2, LE3, LE4, and LE5 spectrometers used standard pulse height analysis (PHA), while ME1, ME2, and TE2 used a first-serve-sampling (FS) technique for pulse height measurements [*Voss et al.*, 1982b]. Most of the LEP spectra have been processed with the FS analyzer because of the higher energy coverage (up to 1000 keV) and the 4-ms sampling period for obtaining the dynamic spectra. The standard PHA had a 64-ms accumulation period. The FS technique is based on the pulse height analysis of the first pulse which exceeds some threshold energy (e.g., 6 keV for TE2) within the 4 ms sampling interval (for ME1 and TE2). This technique preserves the original spectral form. However, for count rates significantly higher than the sampling rate (250 counts/s) only a fraction of the counts are used to generate the spectrum which is therefore statistically limited. The spectrum must then be multiplied by a factor which is derived from the threshold integral counter (scalers). This integral counter registers all pulses above the analyzer threshold during the sampling interval.

The cooled optical photometers on SEEP (AP) were very sensitive to lightning flashes [*Mobilia et al.*, 1985]. Each lightning flash appears as a strong impulse above the background and indicates that thunderstorm activity is present in the troposphere. Because the photometer is looking forward at an angle of 55° from nadir, the lightning is viewed in front of the satellite. The association of these lightning flashes with regions of strong electron bursts was the initial clue for identifying the electron bursts as LEP [*Voss et al.*, 1984].

The fixed-voltage Langmuir plasma probe monitor (PPM) was included to identify ionospheric regions of interest such as the plasma trough, equatorial anomaly, polar cap irregularities, traveling ionospheric disturbances etc. Moreover, because of the large satellite size and non-spherical geometry the plasma probe was also sensitive to strong horizontal electric fields in the direction of the orbit velocity vector. The large length of the conducting satellite is believed to have produced a negative offset voltage of $E_x d$ on the Langmuir I-V characteristic, where d is the distance between the probe and the effective center of the satellite and E_x is the electric field in the direction of travel. Strong electric field transients were observed with this probe in association with the SEEP photometer measurements of lightning flashes [*Voss et al.*, 1984].

The X ray imaging spectrometer (XRIS) used a pinhole-camera technique to form a 7° × 90° cross-track line image of the atmosphere below the satellite on a 16-pixel position-sensitive proportional counter [*Calvert et al.*, 1985]. Auroral activity over a wide area could be observed during each polar pass. This instrument failed after one month in orbit; no X rays produced by LEP striking the atmosphere have been identified in the limited data set available.

3. LEP Observations and Interpretations

3.1. LEP and Wave Data for September 9, 1982

A map showing the locations of six successive nighttime passes of S81-1 during September 9, 1982, is shown in Figure 2 along with the geographic locations of various ground facilities which were involved in the experiment. The dashed sections of the lines indicate locations where the satellite was not recording data. The circled numbers are nighttime orbital pass designations. A series of strong LEP events to be discussed below occurred at the location marked "LEP events" (pass 4). The conjugate location of these events is shown in the southern hemisphere. Lightning flashes were recorded by the AP photometer as indicated over Florida. A weak LEP event was observed off the East Coast of the United States on the previous pass (pass 2). Other locations of interest are Palmer Station in Antarctica, which was the site of a VLF receiver, and the Naval VLF transmitter NAA in Maine.

Figure 3 illustrates the response of the detectors during the orbital pass labeled 3-to-4 in Figure 2. The photometer data in the upper two panels indicate auroral emissions at 391.4 and 630 nm as well as the equatorial anomaly at 630 nm. On the right-hand side, additional optical emissions from cities and lightning flashes appear. The response of the plasma probe monitor (PPM), which gives a measure of the cold plasma density, is shown in the third panel. During this pass the plasma trough in the southern hemisphere is at $L = 3.5$. There are relatively strong plasma irregularities over the midlatitude regions which may be related to the injection of lightning-produced VLF waves [*Carpenter and Colin*, 1963; *Janes*, 1972].

The bottom panel shows locally mirroring electron fluxes (TE2) and precipitating fluxes (LE5) with energy >45 keV. The auroral zone precipitation in the southern hemisphere is on the left of the panel as are the South Atlantic Magnetic Anomaly (SAMA) fluxes. On this pass the trapped radiation was intensified because of a magnetic storm which occurred three days earlier. On the far right-hand side several electron bursts are observed as the satellite passed over the region where the lightning flashes were produced. These bursts will now be described in more detail.

The LEP burst events of pass 4 noted in Figure 3 are displayed on an expanded time scale in Figure 4 where the individual data points, separated by .064 s, are connected by solid lines. The events are labeled A through G and are shown with the simultaneous VLF spectra of sferics and whistlers received at Palmer, Antarctica ($L = 2.3$). These LEP event signatures, which display a rich morphology in the time dependence of the electron counting rates, are interpreted as follows: In passing along the geomagnetic field from north to south a ducted whistler wave from lightning alters the pitch angles of energetic, trapped electrons which are moving northward and whose gyromotion can resonate with the VLF wave. This interaction reduces the pitch angles of some of the electrons, lowers their mirror points to below the satellite altitude, and produces the first electron pulse of the event. Some of these electrons are then magnetically reflected and some are scattered by the atmosphere, resulting in an electron bunch moving to the southern hemisphere where the lower mirroring altitude (due to the South Atlantic Magnetic Anomaly) results in atmospheric contact by the electrons. Some of the electrons are backscattered by the atmosphere and return to the northern hemisphere. Subsequent reflections between the northern and southern hemispheres produce the train of pulses of diminish-

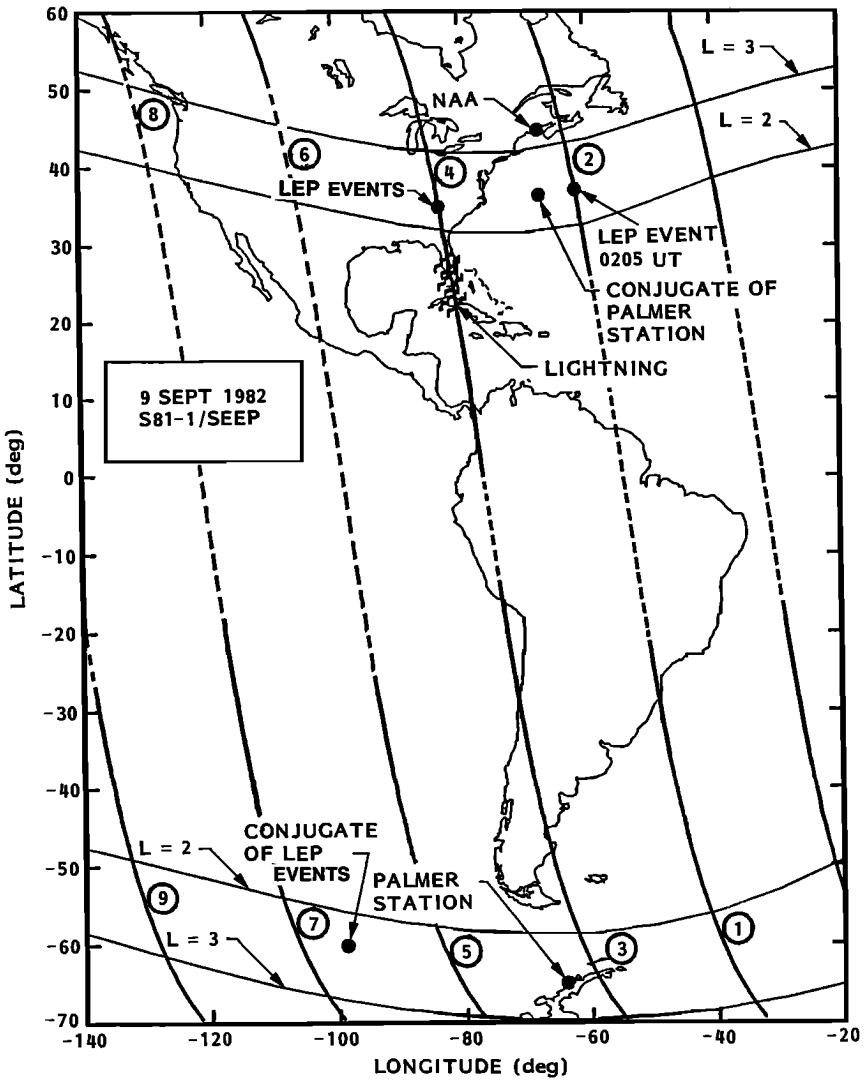

Figure 2. Nighttime orbital passes of the S81-1/SEEP satellite for September 9, 1982.

ing intensity which make up the bunches in the individual events shown in Figure 4.

For the September 9 events, the VLF spectra of lightning generated sferics and whistlers were detected in the conjugate hemisphere at Palmer Station, Antarctica (65° S, 64° W) and are shown at the top of Figure 4. The apparent horizontal line at ~1.9 kHz is due to the well-defined Earth-ionosphere waveguide cutoff frequency. The scaled sferics and whistlers are shown beneath the VLF spectrogram. The dashed portion of a scaled whistler curve is an extrapolation based on the observed solid portion of the curve and the properties of the stronger and more completely defined events such as *F*. The conjugate point of the SEEP location during these events (60° S, 98° W) is 34° to the west of Palmer (see Figure 2), and thus the VLF intensity at Palmer is probably not simply related to the magnetospheric whistler intensity nor to the flux of precipitating electrons. Whistler dispersion techniques [*Carpenter*, 1968] were used to identify the sferics that precede the whistler signals on the VLF spectrogram. Dashed vertical lines denote the times, based on the whistler traces, when the causative sferic should have occurred. An important observation is that the sferic, when identified, preceded the peak of each LEP event by the expected time interval (~0.4 s). The time delay between the sferic and LEP first pulse is equal to the whistler wave propagation time from the atmosphere to the interaction region (near the equatorial plane) plus the time for a trapped electron to travel from the interaction region to the SEEP satellite.

In the strong LEP events, A, D, and E, electron counting rates are observed to increase rapidly to ~100 times background in <200 ms. The envelopes of the individual pulses subsequently decay relatively slowly to background levels over several seconds. Event G is a factor of 10 above background and event F about three times background. Events A and D are shown on expanded scales in Figures 5a and 5b and events F and G in Figure 6. (Events B and C are relatively weak on the integral energy display of Figure 4 but are more prominent in the differential energy spectrum ($120 < E < 140$ keV)). During this pass the TE2 and ME1 detectors were oriented at 89° and 25° respectively to the magnetic field direction. In all LEP events observed at small pitch angles the first peak has lower amplitude than the second. This feature occurs because the wave-particle interaction producing the first peak deflects electrons only a few degrees, whereas the atmospheric scatter-

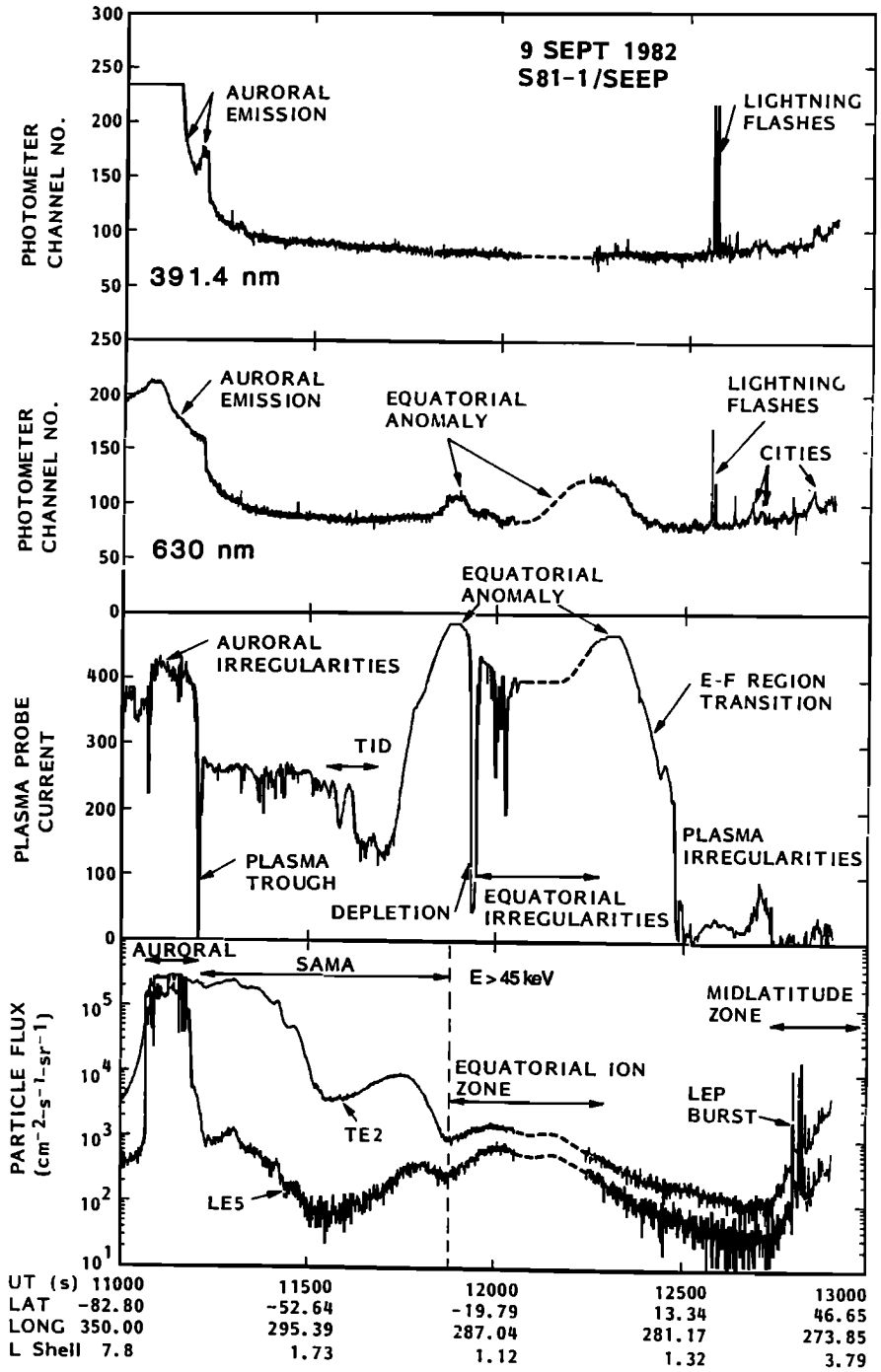

Figure 3. SEEP detector response during a nighttime pass September 9, 1982. Top two panels are photometer data at 391.4 and 630 nm; the third panel is the plasma probe response. The bottom panel shows the particle flux intensities for the TE2 (trapped) and LE5 (precipitating) electron sensors.

ing responsible for subsequent bunches scatters electrons into the entire loss cone.

The flux values of Figures 4, 5a, 5b, and 6 were obtained by dividing the counting rate by the geometric factors of the detectors. However, as will be seen later, the flux distribution varies over the detector acceptance cone. Thus the true directional flux at 89° for the first pulse is somewhat higher than that shown in the figures because the flux did not fill the aperture of the detector uniformly. The relationship between counting rate and directional flux under these conditions is discussed further in section 3.6.

A multiflash lightning sequence is associated with LEP event E. On the basis of the VLF spectrogram, four whistlers with associated sferics occurred within a one second period of time and in the proper time coincidence with LEP event E The absence of a well defined echo pulse structure in the decay portion of the LEP event E is consistent with the occurrence of four closely spaced LEP bursts in which the individual pulses of

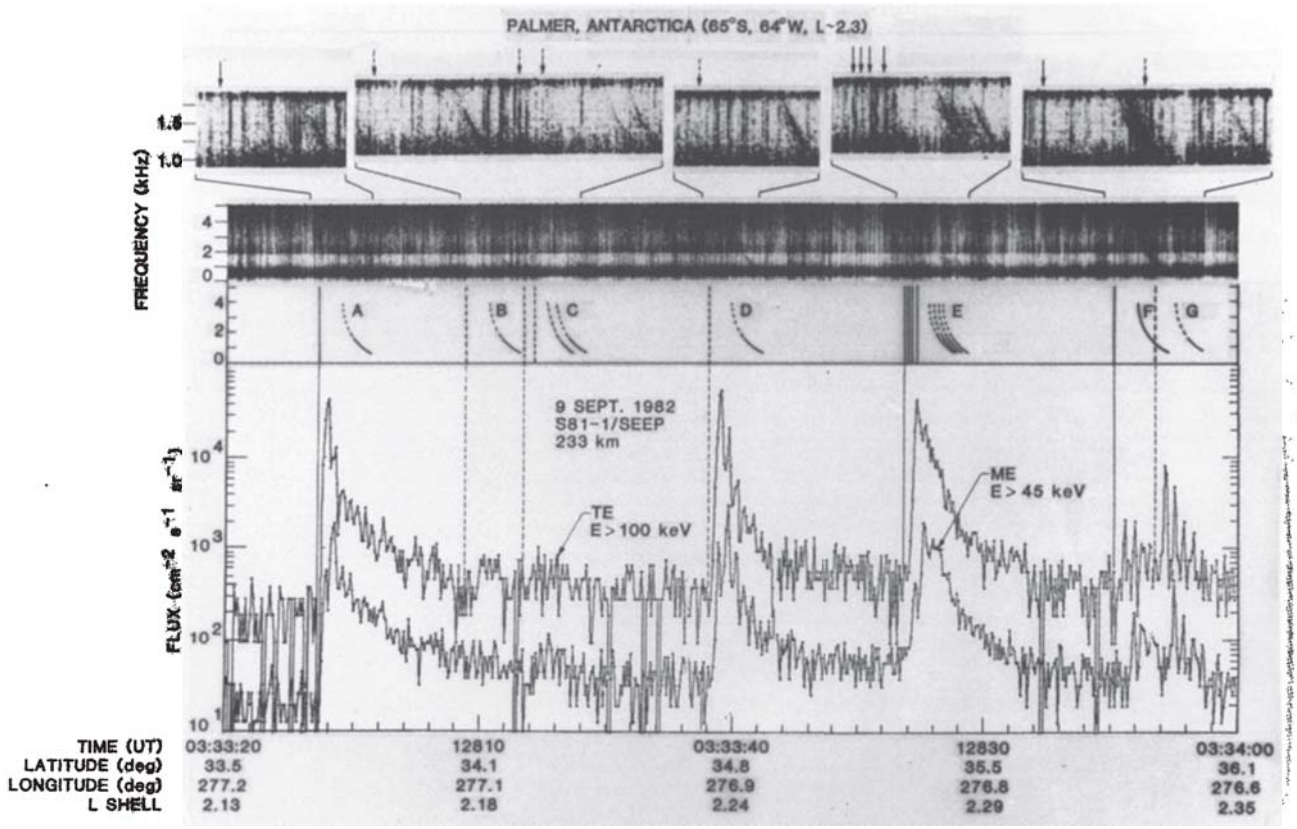

Figure 4. LEP bursts (labeled A to G) recorded with the S81-1/SEEP satellite on September 9, 1982, are correlated one to one with concurrent ground-based VLF whistlers at Palmer Station, Antarctica. Top panels show the VLF spectrograms and the scaled whistlers and sferics. The uppermost insets show the Palmer VLF data with an expanded timescale for the 8 LEP events. The solid lines and arrows represent sferics that were directly identified on these (and other) records, while the dashed lines represent estimates of sferic times based on the dispersion properties of all events. The sampling interval for the energetic particle measurements shown in the lower panel is 64 ms.

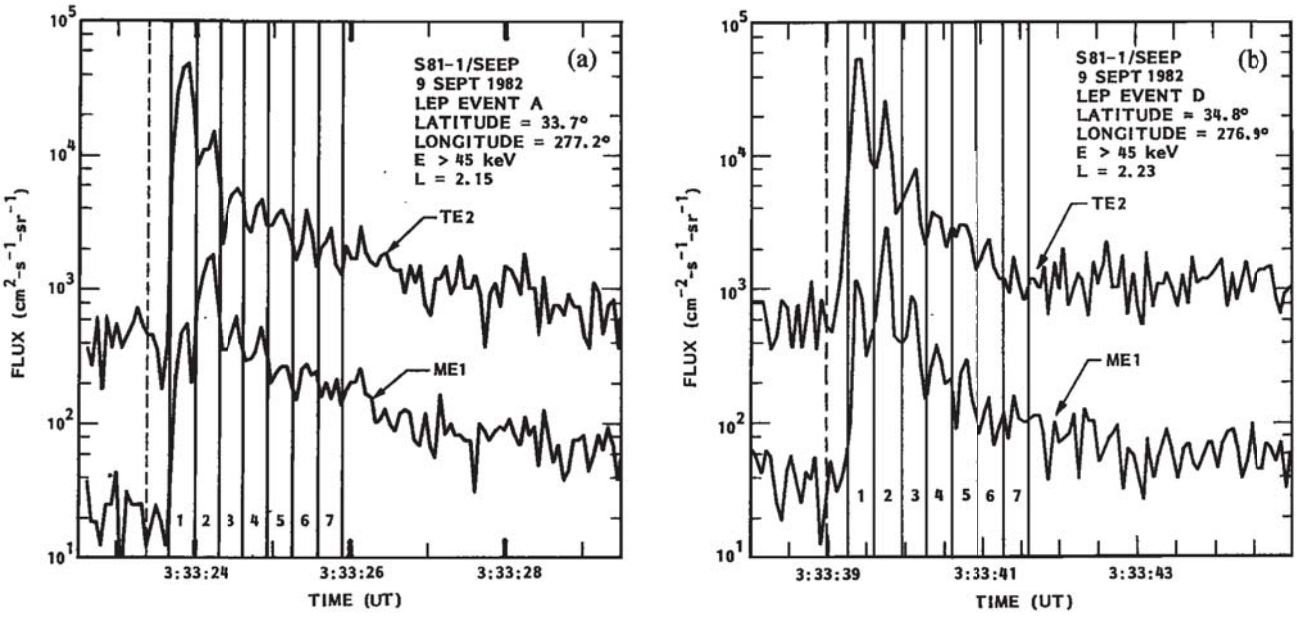

Figure 5. Expanded timescale (a) for LEP event A and (b) for LEP event D of Figure 4.

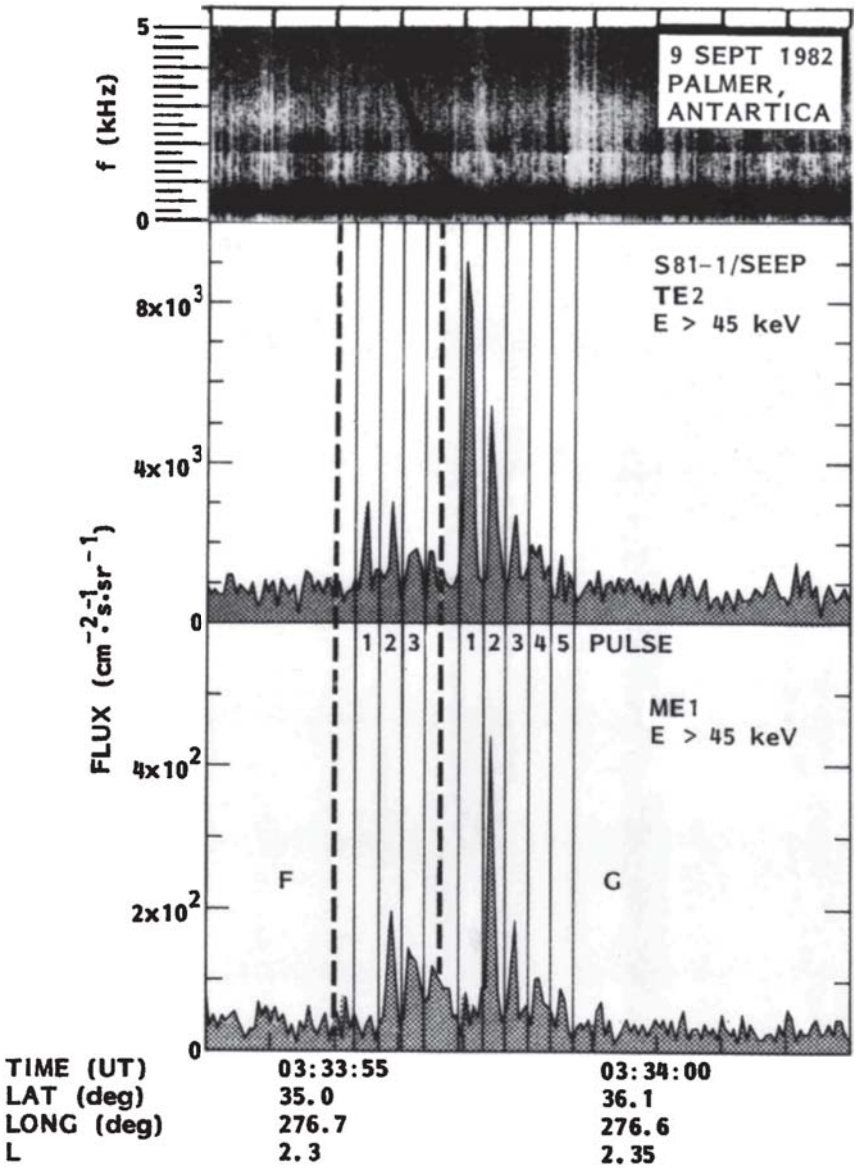

Figure 6. Expanded timescale for events F and G of Figure 4.

bouncing electrons are not in phase. These events indicate that multiflash lightning and its associated whistlers produce overlapping LEP events and that the wave-particle interaction process can respond with superposition of individual impulses spaced as close as 150 ms. The LEP produced by the first of the four strokes is the largest, as might be expected since the first lightning stroke of a multistroke series is often the strongest.

In many years of VLF wave data from the Siple and Palmer stations located in Antarctica, the occurrence of multiflash whistlers is relatively rare. Typically less than 10% of the whistlers that occur within a time interval of 1–2 s exhibit multiple components which show the same dispersion, a signature of propagation via the same path [*Inan and Carpenter*, 1986; D. L. Carpenter, personal communication, 1984]. The whistlers observed at Palmer which are shown in Figure 4 are typical of ducted whistlers propagating in the $L = 2.0$ to 2.5 range. Although these particular whistlers were relatively weak, at Palmer their dispersion characteristics were very similar to much better defined whistlers observed in other episodes at Palmer Station. This fact was used in the analysis of the whistler dispersion profiles for extracting information on the magnetospheric propagation path and the cold plasma density as used by *Inan et al.* [1989].

While the whistlers observed at Palmer and associated with the stronger LEP bursts were not very intense, the sferics received at Palmer for these same whistlers showed relatively high intensity in the 2–4 kHz range. This observation may indicate that the wave energy in the whistlers was strong during the magnetospheric transit but was attenuated while passing through the ionosphere and in the 2000-km-long subionospheric waveguide to Palmer. Also, Trimpi events on the NAA signal, associated with similar whistlers, were observed at Palmer during the 0330–0340 UT period on September 9, 1982. Only one small Trimpi event occurred in association with the LEP bursts observed by the satellite on this pass (event F [see *Voss et al.*, 1984]). For this event the satellite was in the opposite hemisphere from Palmer and the satellite conjugate point was ~2000 km west of Palmer at $L = 2.3$. Since neither

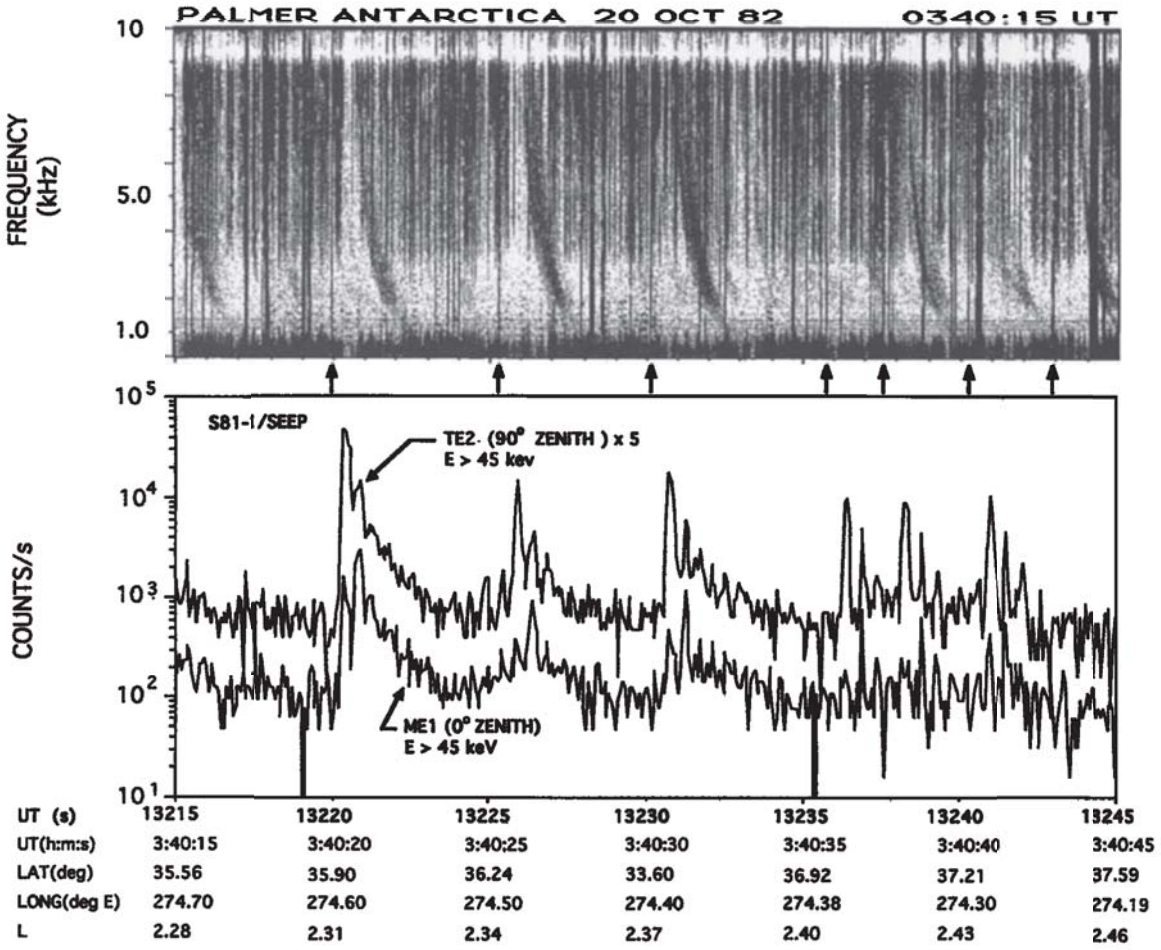

Figure 7. Record of October 20, 1982, showing LEP events over North America correlated with whistlers observed at Palmer, Antarctica.

the satellite nor its conjugate point was close to the great circle path from NAA to Palmer, the LEP observed by the satellite is probably not responsible for the Trimpi event. An additional duct with at least one atmospheric termination on the radio propagation path between NAA and Palmer must have been present. Since the whistler for event F shows multiple traces, additional ducts must be involved.

3.2. Other Examples of LEP Events

Two other examples of LEP burst sequences are shown in Figure 7 for October 20, 1982, and Figure 8 for June 7, 1982. On October 20, six LEP events are well defined, and a whistler and causative sferic can be associated with each LEP [*Imhof et al.*, 1989]. These data were obtained at nearly the same local time (0340 versus 0333 UT) and location (36° versus 35° latitude, 274° versus 277° longitude) as the September 9, 1982, events. An extended time presentation of the October 20 particle and VLF data is shown in Figure 9. During this longer interval the satellite passed from $L = 2.3$ to 3.5. Between $L = 2.3$ and 2.5 the six LEP and correlated whistler events previously shown in Figure 7 occurred. Two additional LEP examples are shown in Figure 9, one near $L = 2.5$ and one at $L = 3.43$. The low-amplitude particle pulses seen between $L = 2.6$ and 3.4 do not have the same time dependence, energy spectra, nor angular distribution of LEP and are presumed to be caused by some other phenomena. It is noteworthy that the strong whistlers which occurred while the satellite was in the interval $2.6 < L < 3.4$ have the same multiduct structure as the ones observed earlier when the satellite was observing LEP at $2.3 < L < 2.55$, yet no electron pulses were correlated with these whistlers. A simple explanation of this sequence is that the satellite passed through the field lines of a duct between $2.3 < L < 2.55$ and observed an LEP each time a

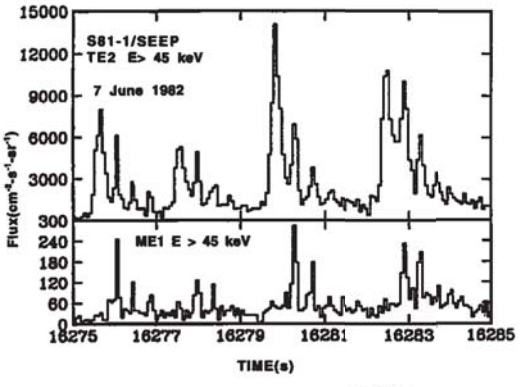

Figure 8. Series of four closely spaced LEP bursts on June 7, 1982.

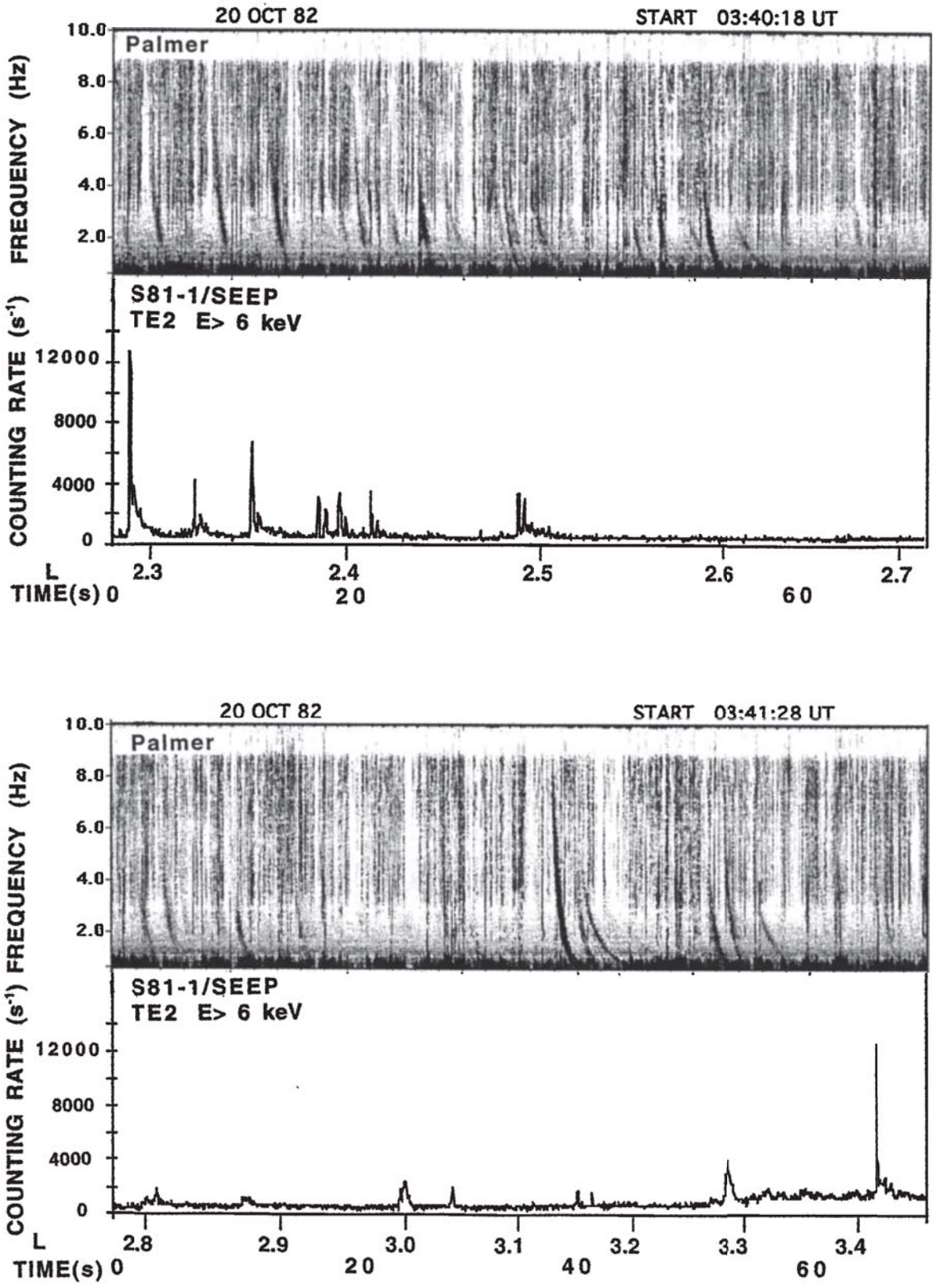

Figure 9. Extended time record of whistlers and LEP events on October 20, 1982.

strong sferic filled the duct with VLF waves. If these six LEP events were formed in the same duct, the latitude extension of the duct would be ~200 km at the satellite altitude. In the interval $2.6 < L < 3.4$ there were no ducts on the field lines traversed by the satellite, so no LEP was detected, even though ducted whistlers occurred repeatedly during this time period. The last LEP in this sequence, at $L = 3.43$ is observed very close to the plasmapause, as measured by the Langmuir probe.

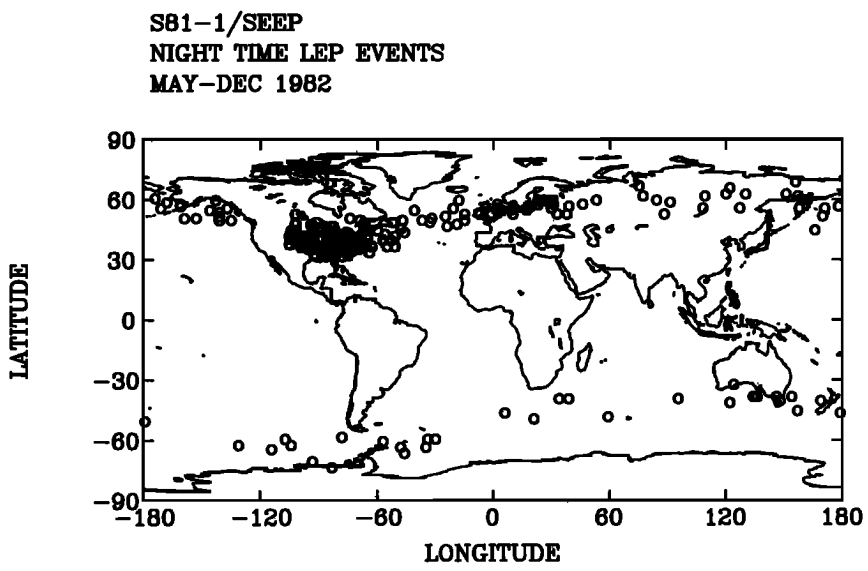

Figure 10. Locations where the SEEP satellite identified strong LEP events during its 6-month lifetime.

This LEP may have resulted from a whistler which was guided by the electron density variations at the plasmapause [*Inan and Bell*, 1977].

For June 7, 1982, a series of four strong LEP bursts separated by ~2.5 s (~20 km) indicates that the duct width or the efficient interaction region projects to a latitude interval of at least 80 km at the satellite altitude. Unfortunately, VLF records from Palmer or Siple were not available for this time. These data also show LEP shape, amplitude, and fine structure which are similar to the September 9, 1982, events. The details of the LEP time structure are discussed in section 3.5. The increase in the ratio of the ME1 and TE2 counting rates after the first pulse is indicative of the broadening of the pitch angle distributions caused by strong atmospheric scattering in the southern hemisphere.

These passes on June 7, October 20, and September 9 are notable in that in each case a series of closely spaced LEPs were observed, the individual LEP pulse train duration being ~2 s and the series lasting for 10–35 s. If LEP is produced by ducted whistlers, then the electron precipitation region corresponds to the projection of the duct onto the atmosphere. In such a series of LEP events, either the satellite was fortuitously beneath a duct each time a whistler occurred or, more likely, a large duct extending perhaps 80 to 300 km in latitude was located above the satellite path. To date there are very few measurements of duct dimensions. *Angerami* [1970] reported observations of whistler waves by the OGO 3 satellite while transiting through ducts at $L = 4.1$–4.7. He obtained duct latitude dimensions which projected to ~25 km at 300 km altitude. *Ikeda et al.* [1988] observed VLF waves with a multistation network and derived duct exit areas with latitude extensions of ~30 km. *Sonwalkar et al.* [1994] detected a ducted ground transmitter wave with receivers on DE 1 and Cosmos 1809. The L shell thickness of the duct was determined to be 55 km at an altitude of 981 km. All of these duct dimensions are significantly less than those required for the LEP signatures of Figures 4, 5, and 6. More recently, *Lev-Tov et al.* [1996] inferred LEP horizontal dimensions in the atmosphere from the characteristics of the transmission anomalies of VLF waves passing near the precipitation site. They concluded that the precipitation pattern was perhaps 300 km in horizontal extent.

The duct modeling work of *Bernhardt and Park* [1977] indicates that the lower boundaries of ducts might extend below 300 km in winter at night. To detect the ducts directly the Langmuir probe data from SEEP were inspected for small increases in plasma density during times when LEP was encountered. Because of the limited accuracy (10%) of the plasma probe and the large density variations associated with the steep lower boundary of the F region, no evidence for ducts was found in the probe records.

3.3. Global Distribution of LEP Events

To date several hundred impulsive, nighttime precipitation events with the general electron flux characteristics of LEP have been identified in the SEEP data. The satellite locations at the times of these detections are shown on a world map in Figure 10. Each symbol denotes a position where one or a series of closely spaced LEP events was observed. The distribution in L of these events is presented as a histogram in Figure 11. Most of the events were observed between L values of 2 and 3, so the detection locations define two bands, one in each hemisphere. This L interval corresponds closely to the slot region in the electron radiation belt. The sampling of SEEP over the globe was not uniform as the payload was actuated more frequently over North America. For this reason and because the radiation background was lower in the northern hemisphere, more LEP was found there. The concentration over the eastern United States is also affected by the strong thunderstorm activity there. The distinct latitude effect is in agreement with the suggestion of *Dungey* [1963] that the frequency range of whistler energy limits the L value over which gyroresonance can occur. *Chang and Inan* [1985] investigated the L range of whistler induced precipitation and identified $2 < L < 3$ as the region of preferred precipitation. The observed upper boundary of LEP near $L = 3$ may also be influenced by the plasmapause, since ducted propagation of whistlers is rare in the low electron density region beyond the plasmaspause [*Carpenter and Sulic*, 1988].

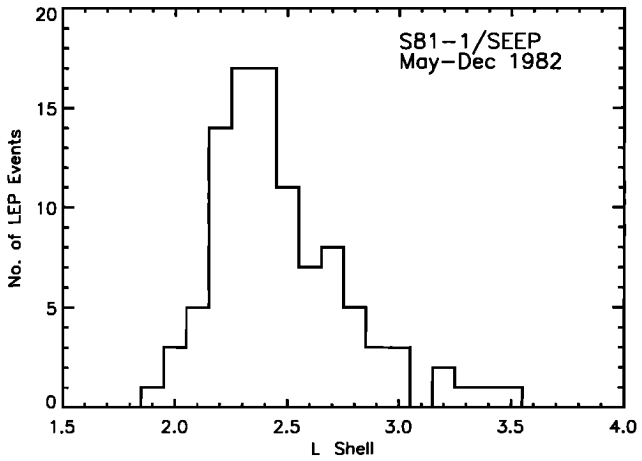

Figure 11. Histogram of the latitude variation of nighttime LEP events.

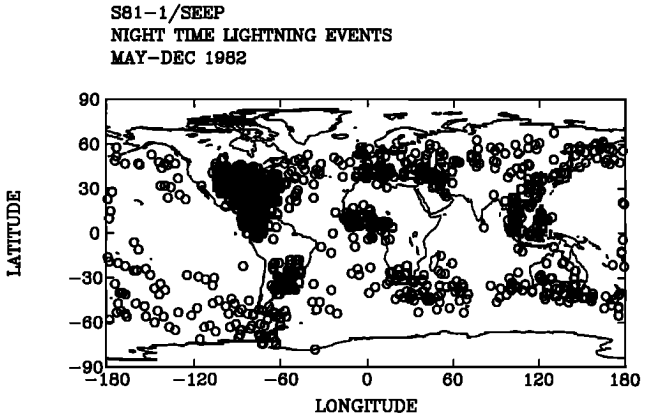

Figure 13. Global distribution of lightning activity observed with the SEEP photometer for May–December 1982.

The airglow photometer of SEEP measured regions of strong lightning activity as illustrated by a sample of photometer data shown in Figure 12. During this 150-s active period the photometer scanned a thunderstorm region, the footprint of the optical sensor being an oval ≈22 km wide by ≈47 km along the track length. During the most intense period lightning flashes occurred within the field of view approximately once per second. The overall global distribution of nighttime lightning flash activity observed with the SEEP photometer (i.e., events similar to those in Figure 12) is shown in Figure 13 where each circle denotes the satellite position when it recorded a cluster of lightning flashes. Lightning activity occurs frequently over the eastern United States and corresponds to the frequent occurrence of LEP activity in that region. However, other concentrations of lightning, such as in Argentina, West Africa, Indo China, and the Philippine Islands do not stimulate appreciable LEP events. These additional lightning sources are at L values below 2 and therefore may not be as effective at producing whistler and LEP as the thunderstorms located in the region between $L = 2$ and $L = 3$.

3.4. LEP Energy Spectra

The differential electron energy spectra for LEP events A, C, D, E, and F of September 9 are shown in the color spectrogram, Plate 1, for the TE2 spectrometer. Electron energies are sorted into 64 channels covering the range of interest from 6 to 400 keV. The three vertical features are events A, D, and E. The spectra exhibit maxima at approximately 150 keV, consistent with cyclotron interactions near the equator. There is some tendency for the spectra of precipitating electrons to become less energetic with increasing L although the statistical uncertainties in these data are too large to allow a firm conclusion. On theoretical grounds one expects the electron energies to decrease with increasing L [*Chang and Inan*, 1985].

The spectra of precipitating electrons shown in Plate 1 are characterized as a broad distribution ranging from perhaps 75 keV to ~300 keV. This spread in energy is to be expected from first-order cyclotron resonance since a range of wave frequencies and a range of electron gyrofrequencies will be involved. The cyclotron resonance simulations of *Inan et al.* [1989] predict an energy distribution between approximately 90 and 300 keV. However, in these computations it was assumed that the whistler wave energy was confined to frequencies below 6 kHz. Components above 6 kHz would precipitate electrons with energies below 90 keV.

During the first precipitation pulse the electron energy spectrum undergoes systematic changes as was illustrated by *Inan et al.* [1989] for event D of September 9. The dynamic spectra for events D and G are illustrated in Figures 14a and 14b, where the lower curves give the structure of the first electron pulse of each event as measured by the TE2 and ME1 scalers. The upper sections of Figures 14a and 14b show the energies of individual electrons sampled by the FS pulse height analyzer. Since the counting rate was much greater than the FS sampling rate, the density of energy points is not related to the flux intensity. In both events the average electron energy increased with time as would be expected since below the nose frequency the whistler frequency decreases with time. To resonate with a

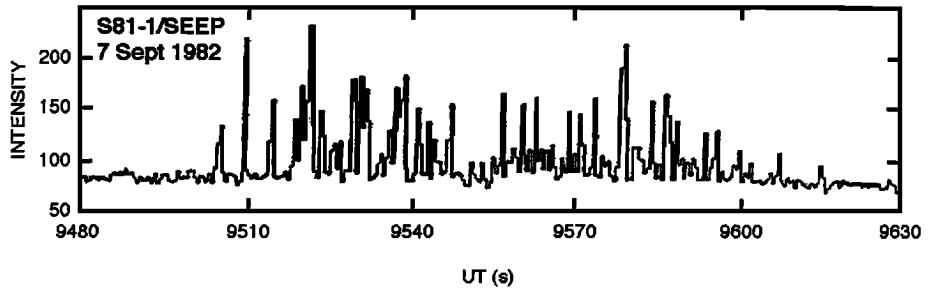

Figure 12. Strong lightning activity observed with the SEEP photometer as the satellite passed over a thunderstorm center. Each impulse represents a lightning flash.

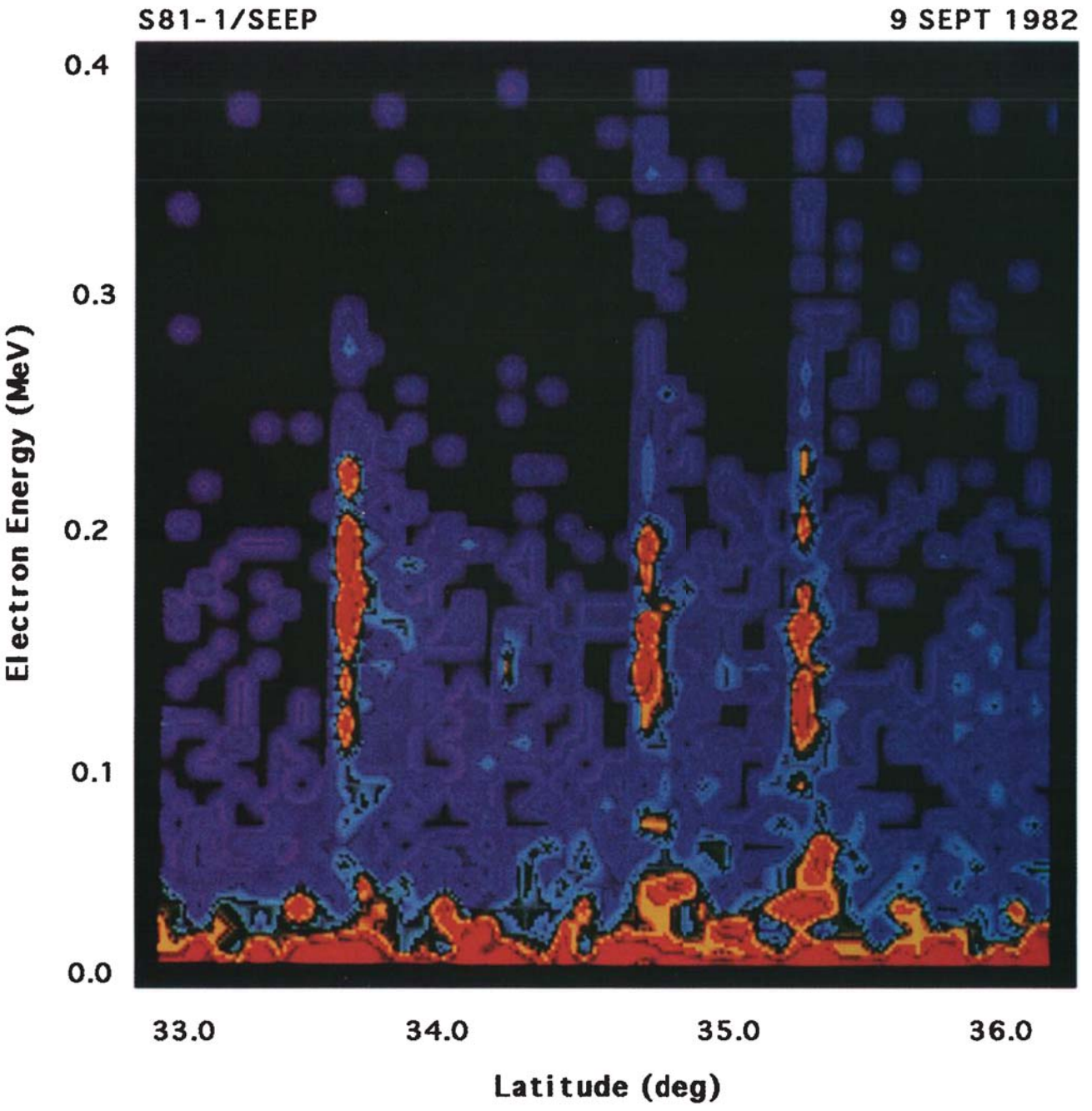

Plate 1. Color spectrogram of the differential electron energy spectra for LEP events on September 9, 1982.

lower-frequency wave the electron must have higher parallel velocity and therefore higher energy.

3.5. LEP Time Structure

Analysis of the temporal structure of the LEP bursts confirms the interpretation that the complex structure of LEP events results from electron precipitation produced by whistler waves. The association of the first peak with electrons scattered by a ducted whistler wave was discussed previously [*Inan et al.*, 1989]. Here we address the overall time structure of the event including the multiple, well-defined echoes. In the temporal structure of LEP events A, D, F, and G (Figure 4), repetitive pulses of nearly constant period and decaying amplitude follow the first LEP peak. Figures 4, 5, and 6 show LEP events on an expanded time scale where the peaks are well defined. The detailed characteristics of the LEP events as seen by the TE2 detector oriented near 90° include the following: (1) the rapid rise and fall of the first electron pulse, (2) the subsequent appearance of equally spaced echoes of diminishing intensity, (3) the relatively slow decay of the pulse envelope, (4) the in-phase and repetitive pulses measured by the TE2 and ME1 detectors, (5) the greater intensity of the flux near 90° pitch angle (TE2) compared with the flux near 0° pitch angle (ME1), and (6) the weak or completely absent first pulse on the ME1 spectrometer (indicating a high ratio of 90° to 25° pitch angle electrons compared with the subsequent echo pulses.

The repetition period of pulses 1–7 in event A of Figure 5a is ~0.32 s. This period is roughly equal to the bounce time of

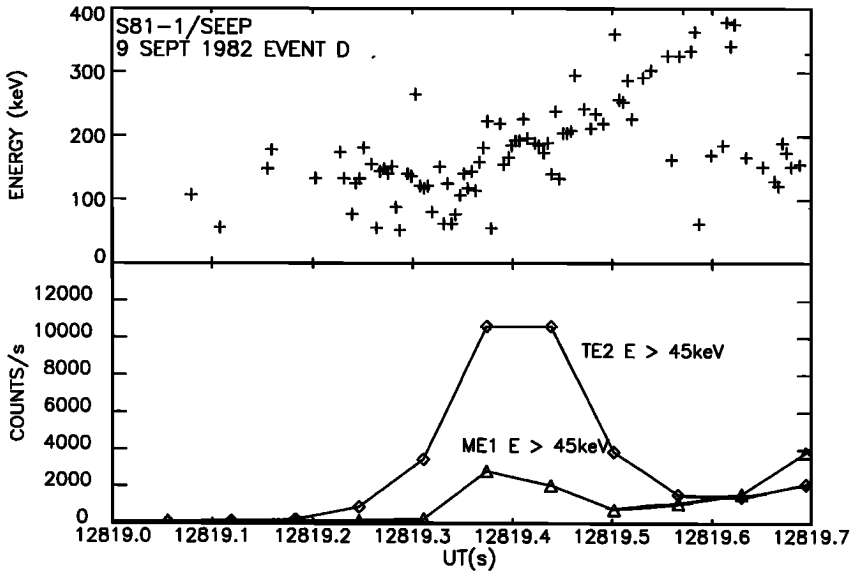

Figure 14a. Dynamic energy spectra and integral counts for event D of Figure 4.

relativistic electrons (~150 keV) echoing between conjugate hemispheres at $L = 2.1$ and with pitch angles near the loss cone angle. For 175 keV electrons the relativistic velocity is $0.67c$ and for 125 keV electrons it is $0.60c$, where c is the speed of light. As the velocity approaches c the bounce period becomes insensitive to the electron energy, hence, velocity dispersion of the electrons during the bounce motion is not significant. For the parameters of event D, about five bounce periods (pulses) should occur before the 175 keV electrons are 180° out of phase with the 125 keV electrons. The pulse period of LEP event G at $L = 2.3$ is 0.38 s. As L increases, the bounce period should increase because of the longer path length and because of a decrease in the parallel resonant velocity.

Although the above arguments make the atmospheric reflection of electron bunches a plausible explanation for the repetitive time structure of LEP events, a quantitative confirmation is needed. In particular, one must demonstrate that enough electrons are backscattered in each hemisphere to sustain the bunches. One must also show that the variations in energy and pitch angle of electrons in a packet will not lead to their rapid dispersion. To investigate these effects a simulation of the time history of event D was done by the Monte Carlo method. An initial distribution of electrons was constructed with a time history equal to the first pulse of event D and with energies that varied with time as depicted by the solid line fit to the electron energy points of Figure 14a. Electrons drawn at random from this distribution were traced through repeated north-south bounces. After each atmospheric encounter the energy and pitch angle of the reflected electron was chosen by random selection from the expected distribution of backscattered electrons.

The basic atmospheric backscatter data for the fraction

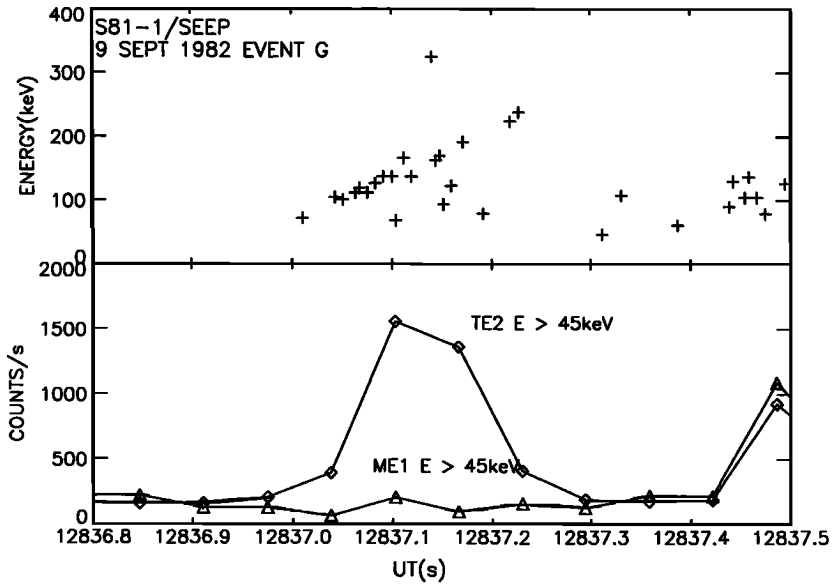

Figure 14b. Dynamic energy spectra and integral counts for event G of Figure 4.

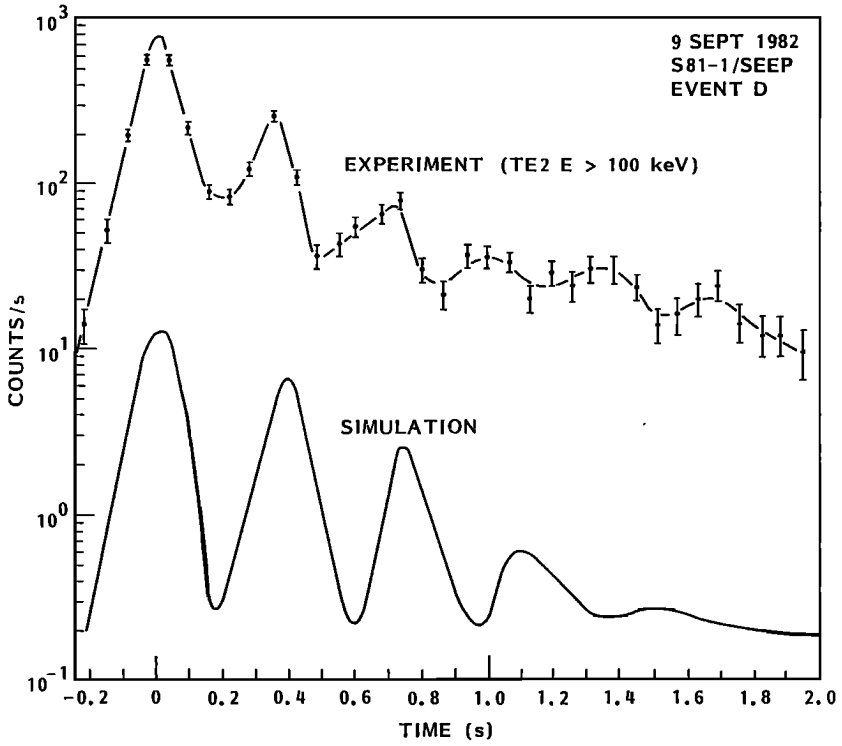

Figure 15. Comparison of Monte Carlo simulation of LEP event D for September 9, 1982 with observed electron pulse sequence. Simulation results are displaced downward for easier comparison.

backscattered, the energy loss, and the pitch angle changes were taken from the results of *Stadsnes and Maehlum* [1965] and *Maehlum and Stadsnes* [1967], who investigated the characteristics of auroral electrons reflected by the atmosphere. For a selection of incident energies and pitch angles, their results give the backscattered electron energy spectrum and pitch angle distributions. In the present simulation their data for an incident electron energy of 100 keV were used. Since they only considered incident pitch angles of 30°, 60°, and 80°, interpolations and extrapolations were made to give a full range of incident angles for the present calculation. Their results show that for electrons with energies between 20 and 100 keV striking the atmosphere at 80° zenith angle, ~70% are backscattered. This reflection percentage drops to 18% for zenith angles of 30°. The energy spread of the backscattered electrons is a broad distribution extending between approximately 70% and 100% of the incident energy but with an average energy loss of ~10%. In the present calculation the bounce time was computed assuming a dipole magnetic field but taking into account the relativistic velocity and the pitch angle of individual electrons during each bounce. Electron energy and time of arrival were recorded each time an electron reached the satellite location in the northern hemisphere. Integrating these data over energies above 45 keV then gave a time varying flux which could be compared with the observed counting rates.

The comparison of model results with data is shown in Figure 15 where the upper curve is the same experimental data given before in Figure 4 although in this case individual data points are plotted with statistical errors. The simulation results are given by the lower curve which includes a steady background rate equal to 1.5% of the counting rate of the initial peak. This background level is the same as that observed in the experiment. The Monte Carlo simulation is in good agreement with the observed time variation. The times of arrival of the pulses are accurately reproduced and the burst coherence persists for five to six pulses. Also, the amplitude decrease between successive pulses is similar to that observed. This agreement, even allowing for the approximations in the simulations and the uncertainties in the initial spectrum, confirms the interpretation that the time structure of LEP events results from repeated reflections of an electron bunch.

A detailed examination of the processes involved reveals that several factors contribute to maintaining the integrity of the electron packet. The energy variation of the initial pulse, in which the most energetic electrons arrive later, allows the faster electrons to overtake the slower ones, thus compressing the time duration of the pulse. In the atmospheric reflection process the electrons backscattering at the smaller pitch angles (more nearly parallel to the field line) have, on the average, experienced more individual collisions and have lost more energy. However, their shorter spiral path to the opposite hemisphere compensates to some extent for their lower velocity. These effects reduce the dispersion expected from velocity and helical path length differences and help maintain the bunch coherence.

The first echo from the southern hemisphere occurs ~0.4 s after the initial pulse. All of these returning electrons were scattered by the atmosphere in the south. Hence an ionization pulse at the southern conjugate point must have occurred ~0.2 s after the initial ionization pulse in the north. This near-simultaneous (<1 s) Trimpi event production at conjugate points was noted by *Burgess and Inan* [1993]. In a recent paper, *Faith et al.* [1997] suggest that the coincident conjugate Trimpi events are evidence for chaotic scattering near the equatorial plane. While strong scattering may occur and is a possible explanation for the broad angular distribution of scattered

electrons, it is not required to produce the near-simultaneous conjugate ionization pulses.

3.6. Electron Loss Rates From Ducted Whistler Waves

The LEP events described in the previous sections are direct evidence that lightning discharges cause a loss of electrons from the radiation belts. Furthermore, the tendency of LEP events to cluster in the slot region of the electron belt suggests that LEP may play a role in controlling the trapped electron population. The influence of whistler waves on trapped electrons has been noted by *Dungey* [1963], *Cornwall* [1964], and *Roberts* [1969], and theoretical estimates of the importance of this mechanism have been made. Most of the early work was hampered by a lack of information on whistler wave intensities and occurrence rates. However, on the basis of a major disagreement between computed and measured pitch angle distributions, *Roberts* [1969] concluded that ducted whistlers were not an important loss mechanism. Other authors have focused on the effects of waves from plasmaspheric hiss [*Kennel and Petschek*, 1966; *Lyons et al.*, 1972] and from high-power VLF transmitters [*Vampola*, 1983].

The importance of the LEP mechanism in the overall structure and intensity of the electron radiation belt and the influence of energy deposition which occurs in these events on the ionosphere and atmosphere depend on the frequency of LEP occurrence and on the number of electrons precipitated in each event. In this section we estimate the number of electrons lost during a single LEP event (event D in Figure 4) based on the electron flux measurements. We then use this result to make an assessment of the importance of ducted whistlers in removing electrons from the radiation belt.

The basic data available on electron losses consists of the counting rates as a function of time for electron spectrometers oriented at three pitch angles. These data specify the differential, directional electron fluxes which, combined with the magnetic field model, yield the number of electrons entering the atmosphere. At the satellite location in the northern hemisphere at an altitude of 280 km the conjugate point in the southern hemisphere is ~50 km below sea level. Therefore the SEEP detectors cannot directly observe all of the precipitating electrons and an extrapolation is needed to obtain the total electron loss. A further complication arises from the fact that the pitch angle spread of the electron flux is comparable to the acceptance angle of the detector collimators, thus requiring an unfolding computation to estimate the electron pitch angle distribution.

All of the electrons measured by SEEP during the LEP events will encounter the dense atmosphere either below the satellite or at the conjugate point during their next half bounce. Hence it is expected that all electrons observed in the first pulse of a LEP event will precipitate in either the northern or southern hemisphere during the next few seconds. Those electrons involved in subsequent bounces within an event are (with the exception of electrons mirroring within ~150 km above SEEP) the same electrons seen in the initial pulse and should not be included again in the total electron loss calculation.

If $j(\alpha, E, t)$ is the differential, directional electron flux as a function of pitch angle α, ($\alpha = 0$ is downward along the field line) energy E, and time t, the number of electrons passing through a square centimeter perpendicular to B during a LEP pulse is given by

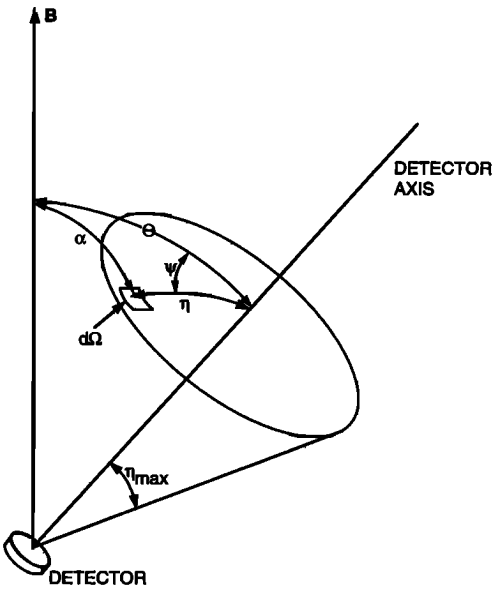

Figure 16. Geometry of detector aperture and magnetic field orientation for calculating sensor response to nonisotropic flux.

$$N = 2\pi \int_0^T dt \int_{E_1}^{E_2} dE \int_0^{\pi/2} j(\alpha, E, t) \cos\alpha \sin\alpha \, d\alpha \qquad (1)$$

where the time integral is taken over the first pulse, of duration T, the energy integral is over the range of interest and the angular integral is over the downward hemisphere. The flux is assumed to be gyrotropic, i.e., $j(\alpha, E, t)$ is not a function of the gyrophase angle. This integral can be evaluated directly once the flux distribution $j(\alpha, E, t)$ is obtained. The fluxes observed in the first pulse by the SEEP detectors are highly anisotropic, the intensity being largest near 90° pitch angle. Since the detector acceptance angles are wide (20° conical half angle for TE2 and LE5 and 30° for ME1) compared to the flux distribution, the relation of counting rate to flux is given by an integral of the flux over the aperture of the detector. In Figure 16, B is a vector pointing upward antiparallel to the magnetic field, and the axis of the detector is oriented at an angle, Θ, to the magnetic field. The element of solid angle for the detector aperture is $d\Omega = \sin\eta \, d\eta \, d\Psi$, where η is the off-axis polar angle and ψ is the azimuthal angle around the detector axis measured from the plane containing the detector axis and B. Since the detector sensitivity is axisymmetric, the detector counting rate $dN(E)/dt$ for electrons of energy E within unit dE is

$$\frac{dN(E)}{dt} = \int_0^{2\pi} \int_0^{\eta_{max}} j(\alpha, E) A(\eta) \sin\eta \, d\eta \, d\Psi \qquad (2)$$

where η_{max} is the limiting acceptance angle of the detector and $A(\eta)$ is the effective area. The pitch angle α is a function of η, Θ, and ψ, the relationship of these quantities being given by the cosine law for spherical triangles.

$$\cos\alpha = \cos\eta \cos\Theta + \sin\eta \sin\Theta \cos\Psi \qquad (3)$$

The shape of the angular distribution was obtained by parameterizing the electron distribution and calculating the

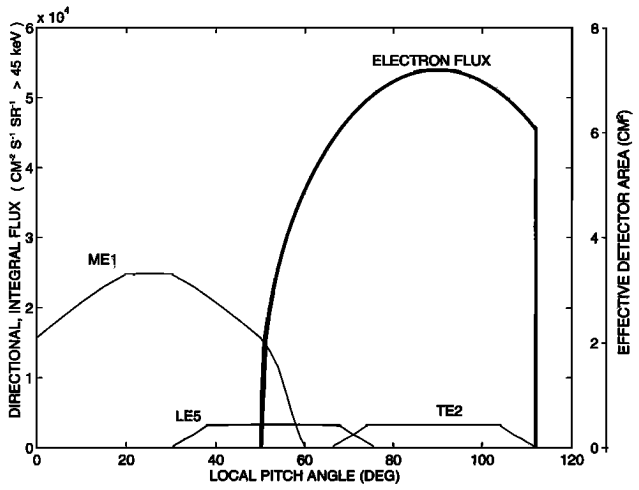

Figure 17. Best fit obtained for directional electron flux of >45 keV electrons scattered by whistler. At this altitude (200 km), electrons with pitch angles <68° will enter the atmosphere at 100 km.

counting rate of the three detectors using (2). The pitch angle distribution was assumed to be of the form

$$j(\alpha) = [\cos m(\pi/2) - \alpha]^n \tag{4}$$

$$\frac{\pi}{2}\left(1 - \frac{1}{m}\right) < \alpha < \frac{\pi}{2}\left(1 + \frac{1}{m}\right)$$

and zero elsewhere.

The parameters m and n were adjusted to fit the observed counting rates, the best fit being obtained with $m = 2.25$ and $n = 0.4$. Figure 17 is a plot of the electron pitch angle distribution as obtained by this method. No electrons are included beyond 112° as these upward-going electrons would have encountered the atmosphere below 100 km altitude. The geometric factors of the TE2, ME1, and LE5 detectors are also shown to indicate the sensitivity of the detector array to the pitch angle distribution. Electrons with pitch angles less than 68° will mirror below 100 km in the northern hemisphere. Since the conjugate point of the satellite is below sea level in the southern hemisphere all electrons detected here will encounter the atmosphere in the southern hemisphere.

The angular distribution at the satellite altitude was transformed into the angular distribution appropriate to an altitude of 100 km in the conjugate region using Liouville's theorem. After this transformation it was necessary to extrapolate the distribution for $\alpha > 75°$ as these pitch angles represent electrons mirroring above the satellite. This extrapolation to large α does not introduce significant error in the number precipitating as the flux is weighted by $\cos\alpha$ in (1) to find the number of precipitated electrons. The resulting pitch angle distribution was inserted into (1) and integrated over angle, energy, and time for the first pulse to give the number of electrons lost through a one cm^2 area perpendicular to the field line at 100 km. For event D and electron energies above 45 keV, the electron loss in this LEP event is $N(E > 45 \text{ keV}) = 7.4 \times 10^3$ electrons cm^{-2}.

It is of interest to compare this loss figure with the inventory of electrons with $E > 45$ keV normally in a flux tube at $L = 2.15$. The number of electrons of energy greater than E_1 in a magnetic tube one square centimeter in area at the equatorial plane is given by

$$N_t(E > E_1) = \int_{E_1}^{\infty} dE \int_0^{\pi/2} j_{eq}(\alpha_{eq}, E)\tau_b(\alpha_{eq}, E)2\pi \cos\alpha_{eq} \sin\alpha_{eq}\, d\alpha_{eq} \tag{5}$$

where j_{eq} is the differential, directional flux in the equatorial plane and $\tau_b(\alpha_{eq}, E)$ is the full bounce period. The number of electrons in a tube having unit area perpendicular to B at the top of the atmosphere is obtained by multiplying the equatorial inventory from (5) by the ratio of the magnetic field values at the 100 km level and at the equator. This ratio is ~9.2 for $L = 2.15$. Using the flux values and formulas listed for the AE-5 Inner Zone Electron Model [*Teague and Vette*, 1972] the total number, N_t, of electrons above 45 kev in a magnetic tube having one square centimeter cross section perpendicular to B at 100 km is $N_t = 4.8 \times 10^8$. Therefore the fraction of electrons in the flux tube which is precipitated in a single LEP event is 1.5×10^{-5}. Note that this loss only occurs in the flux tube where the wave-particle interaction takes place.

The trapping lifetime of electrons in the energy range subject to removal by ducted whistlers was estimated by *Burgess and Inan* [1993]. They expressed the mean lifetime τ of a trapped electron in terms of the fraction $(\delta n/n) \approx 1.5 \times 10^{-5}$ which would be removed from a flux tube by a single ducted whistler.

$$1/\tau = (\delta n/n)WD(A_d/A_s) \tag{6}$$

where $W \approx 0.1$ s^{-1} is the average occurrence rate of ducted whistlers as observed from Port Lockroy, Antarctica, and $D \approx 10$ is the number of ducts excited by each whistler. A_d is the area of a duct projected along magnetic field lines onto the upper atmosphere, and A_s is the area of the upper atmosphere between $L = 2$ and $L = 3$ which was monitored for ducted whistlers to obtain the whistler rate W. For ducts 11 km in radius $A_d = 370$ km^2. The area monitored A_s was computed by Burgess and Inan to be 6.6×10^6 km^2. With these values $\tau = 5 \times 10^4$ days. Since the observed lifetime of electrons at $L = 2.2$ is a few weeks, it appeared that the direct removal of trapped electrons by ducted whistlers was not an important loss process even if the duct radius was much larger than the assumed value of 11 km.

However, in addition to the direct precipitation of electrons in an LEP event, whistler waves alter the pitch angles of the trapped electrons, leading to pitch angle diffusion and eventual loss. While this slow diffusion is less dramatic than the direct precipitation in an LEP event, the cumulative effect of diffusion may be more important. If μ is the cosine of the equatorial pitch angle of an electron and the diffusion coefficient $\langle(\Delta\mu)^2\rangle/2$ is assumed to be independent of μ, the lifetime τ is related to the smallest eigenvalue of the pitch angle diffusion equation [see *Schulz and Lanzerotti*, 1974, pp. 77–78].

$$1/\tau = (1/2)\langle(\Delta\mu)^2\rangle(2.3/\mu_c)^2 \tag{7}$$

The factor $(2.3/\mu_c)^2$ results from requiring the flux to be equal to zero at μ_c, the cosine of the loss cone angle.

The quantity $\langle(\Delta\mu)^2\rangle$ is the ensemble average of $(\Delta\mu)^2$ per unit time, where $\Delta\mu$ is the change in the pitch angle cosine of an electron caused by scattering from the whistler wave. This

quantity was obtained by *Burgess and Inan* [1993] for whistler waves of 12-pT intensity by scaling the trajectory calculations of *Inan* [1987] to 12 pT and $L = 2.24$. Here $(\Delta\mu)^2$ will be estimated independent of any theoretical model of the wave-particle process by using the measured pitch angle distribution of LEP electrons. Making the extreme assumption that the initial distribution function f_0 is constant outside the loss cone and zero inside, the pitch angle distribution f_1 within the first pulse of an LEP is

$$f_1(\mu) = \int_{-|\Delta\mu_{max}|}^{|\Delta\mu_{max}|} f_0(\mu - \Delta\mu) P(\Delta\mu, \mu - \Delta\mu)\, d\Delta\mu \quad (8)$$

where $P(\Delta\mu, \mu - \Delta\mu)$ is the probability that the whistler wave will cause a particle at $\mu - \Delta\mu$ to change its pitch angle cosine by $\Delta\mu$ within unit $\Delta\mu$. It is assumed that only small angle scattering occurs so that $P(\Delta\mu)$ is negligible for $|\Delta\mu| > 1 - \mu_c$. Several parametric expressions for $P(\Delta\mu, \mu - \Delta\mu)$ were assumed, such as $P(\Delta\mu) = (1/g)(1 - |\Delta\mu|/g)$ for $|\Delta\mu| < g$ and $P(\Delta\mu) = (\pi/4g) \cos(\pi\Delta\mu/2g)$ for $|\Delta\mu| < g$, and values of the parameter g were adjusted to give $f_1(\mu)$ having the same width as the observed LEP distributions derived by fitting (4). With these values of $P(\Delta\mu)$ the average change in $(\Delta\mu)^2$ for interacting electrons is found to be

$$(\Delta\mu)^2_{ave} = \int_{-\Delta\mu_{max}}^{\Delta\mu_{max}} (\Delta\mu)^2 P(\Delta\mu) d(\Delta\mu) = 5 \times 10^{-5} \quad (9)$$

This value of $(\Delta\mu)^2_{ave}$ is too large because all energetic electrons in the flux tube do not pass through the interaction region at the time the wave amplitude and frequency are most effective for scattering. The investigation of *Inan et al.* [1989] found that most of the scattering took place within 5° of the equator. A whistler pulse at 4 kHz passes through such a region in ~0.1 s, which is one half the bounce period of a 100 keV electron at $L = 2.2$. Hence only half the electrons in the tube are affected and $(\Delta\mu)^2_{ave}$ as calculated from (9) should be multiplied by 1/2.

The ensemble average $\langle(\Delta\mu)^2\rangle$ needed for (7) is the time average of $(\Delta\mu)^2_{ave}$ and its calculation requires a knowledge of the occurrence rate of ducted whistlers and the probability of a given electron being in a duct at the time a whistler passes along the duct.

$$\langle(\Delta\mu)^2\rangle = (\Delta\mu)^2_{ave} WD(A_d/A_s) \quad (10)$$

where W, D, and (A_d/A_s) are the same quantities introduced in (6).

Using $(\Delta\mu)^2 = (1/2)\ 5 \times 10^{-5}$ and an assumed duct radius of 25 km at 100 km altitude results in $\tau = 360$ days, still much larger than observed values. However, this result is sensitively dependent on the duct radius. If the average duct radius is ~100 km, the electron lifetime from interactions with ducted whistlers would be 22 days, which is comparable to the observed lifetimes.

For simplicity, it has been assumed here that the cross section of a duct is circular. The analysis of *Angerami* [1970] and *Ikeda et al.* [1988] suggest that the longitude extent of a duct may be several times the latitude width. The lifetime values calculated here depend on the projected area of a duct and not on the geometrical shape. The assumption stated just before (8), that the initial electron distribution is uniform outside the loss cone and zero inside, leads to an underestimation of the loss rates from LEP. In reality the pitch angle distribution has a finite slope near the loss cone. Such a distribution in (8) would lead to a larger $P(\Delta\mu, \mu - \Delta\mu)$ and a larger $\langle(\mu)^2\rangle$. However, the distribution function f_0 is not well known, and the assumption used here is adequate for the current estimates.

A limitation in these estimates is the fact that $\langle(\mu)^2\rangle$ was evaluated near $\mu = \mu_c$ and was assumed to be independent of μ. From the SEEP data it was not possible to measure the scattering rate at any angles other than near the loss cone angle. Theoretical estimates of the wave-particle interaction process find that scattering rates become smaller for large equatorial pitch angles, a condition which led *Roberts* [1969] to discard lightning produced whistler waves as an important diffusion mechanism. The present results indicate that ducted whistlers may cause important losses of electrons in the slot region of the magnetosphere, but additional mechanisms, such as interactions with hiss, chorus, or transmitter emissions, will be required to feed equatorially trapped electrons to lower pitch angles where ducted whistlers can interact effectively.

3.7. Role of Ducted and Nonducted Whistlers in the Production of LEP

The interpretation of the LEP observations has been based on the interaction of trapped electrons with ducted whistlers, although nonducted whistler waves occur more frequently in the region of the plasmasphere where LEP is encountered. The assumption that ducted waves are responsible is based both on the strong association of ducted whistlers with LEP [*Burgess and Inan*, 1993] and on the agreement between the observed characteristics of the precipitating electrons and the properties computed on the basis of electron scattering by ducted whistlers [*Inan et al.*, 1989].

In most of the cases where SEEP electron bursts have been compared with wideband VLF data from ground stations, ducted whistlers were found to accompany LEP. Many cases of ducted whistlers were found for which no LEP was observed, but this result is expected since the satellite was seldom located beneath a duct and in a position to observe the LEP. In a similar comparison using VLF propagation anomalies to detect precipitation, *Burgess and Inan* [1993] found 23 Trimpi events in a 10-min interval. For each of these events they were able to identify a ducted whistler at the correct time, and arriving from the correct direction, to produce the LEP.

The analysis of the time dependence of the LEP pulse and the dynamic energy spectra of the precipitating electrons also supports the contention that ducted whistlers are responsible for the precipitation. *Inan et al.* [1989] analyzed a single LEP event occurring at $L = 2.24$ and showed that the observed electron spectra, time dependence, and intensity were in agreement with electron characteristics expected from the interaction of trapped electrons with ducted whistlers. While this agreement does not preclude precipitation from nonducted whistlers it does support the argument that ducted waves are the cause of the well-defined, structured events discussed in this paper. In particular, the energies of the precipitating electrons calculated by *Inan et al.* [1989] were in excellent agreement with observations. Ray tracing computations of nonducted VLF waves inside the plasmasphere show that the wave normal angle becomes large (≈60°) by the time the wave reaches the equator [*Strangeways and Rycroft*, 1980]. The condition for first-order resonance for a whistler mode wave then becomes

Table 2. Resonant Energies

Frequency, Hz	$\psi = 0$	$\psi = 50°$	$\psi = 70°$
500	829 keV	1108 keV	1633 keV
1000	493	675	1018
2000	276	386	695
4000	142	201	312

$$\omega + \omega n(\omega, \psi, \Omega, n_e) \frac{v_{res}}{c} \cos \psi \cos \alpha = \Omega/\gamma \quad (11)$$

where ω is the wave angular frequency, $n(\omega, \psi, \Omega, n_e)$ is the index of refraction of the ambient cold plasma, ψ is the wave normal angle, Ω is the electron gyrofrequency, n_e is the cold plasma density, v_{res} is the velocity of the resonant electron, α is the electron pitch angle, and γ is the relativistic mass increase factor. Solving this quadratic equation for v_{res}/c for the conditions of the LEP event designated as D for September 9, 1982, one obtains the following values of the equatorial resonant energies shown in Table 2.

While a complete particle simulation of trapped electron scattering by nonducted whistler waves is clearly needed, it is apparent from Table 2 that resonance energies for nonducted waves are higher than those for the ducted case. Since the calculation for the ducted case is in good agreement with experiment, one would expect that a similar computation for nonducted waves would not agree with observations.

The time delay between the lightning flash and the arrival of electrons at the satellite altitude is a sensitive measure of the interaction phenomena. Since the wave velocity is less than the electron velocity, the major part of the time delay is due to the wave transit time to the altitude where resonance occurs. One would expect this time delay to increase with L in a predictable way. The October 20, 1982, pass of S81-1 over North America displayed in Figure 9 observed a series of 8 LEP events on L values ranging from 2.3 to 3.43. Ducted whistlers were identified for each of these events in broadband VLF records from Palmer Station, Antarctica, and the causative sferics were found. For the LEP at $L = 3.43$, the ducted whistler was weak and two possible sferics, separated by 0.04 s were found. The time delays between the sferics and the arrival of the peak values of the electron bursts are plotted as a function of L in Figure 18. The monotonic increase in the time delay with L is expected primarily from the increase with L of the path length from the ionosphere to the resonance region. The large error in the time delay indicated for the LEP at $L = 3.43$ results from the ambiguity in the sferic identification.

The solid curve of Figure 18 represents calculated values for the time delay obtained by *Chang and Inan* [1985] using the test particle code to simulate the interaction of a ducted whistler wave with the trapped electron population. Chang and Inan assumed an electron density which was less dense than an average plasmaspheric density constructed by *Carpenter and Anderson* [1992] from DE 1 satellite measurements. Therefore the original delay times of Chang and Inan have been adjusted to the Carpenter and Anderson plasmaspheric density by assuming that the wave transit time is proportional to $[n_{eq}]^{1/2}$. Although the absolute values of the time delays depend on the unknown electron densities, the variation of the delay with L should follow the predictions. On this point the experimental values and calculated values both show a similar L dependence. If the actual electron densities on October 20 were a factor of 2 higher than the average values assumed here, the agreement would be within measurement errors.

4. Conclusions

In this paper we have described the characteristics and some of the consequences of lightning-induced electron precipitation. Previous studies of the global distribution of LEP events, the dimensions of the precipitation regions, and the frequencies of LEP occurrence have been based on the detection of VLF propagation anomalies in the Earth-ionosphere waveguide [*Inan et al.*, 1988; *Burgess and Inan*, 1993; *Lev-Tov et al.*, 1996]. The results presented here are derived from direct measurements of the precipitating electrons.

The outstanding features of LEP as observed between $L = 2$ and $L = 3$ are summarized below.

1. The basic signature of LEP is a short pulse of precipitating electrons with energy 100 keV $< E <$ 300 keV and a duration of ~0.2 s. This pulse is followed by a train of pulses formed as the electron bunch alternately reflects between the northern and southern hemispheres. This electron signature is consistent with the precipitation expected from pitch angle scattering of trapped electrons by a ducted whistler wave produced by a lightning flash.

2. Well-defined LEP events occur primarily in the plasmasphere between $L = 2$ and $L = 3$. In the SEEP data, LEP was found more often in the northern hemisphere over the eastern United States. This observed concentration results from the lower radiation background, the frequent lightning occurrence, and the more concentrated data acquisition which took place in that region. However, the greater data sampling rate over North America did not significantly distort these findings since the world wide lightning distribution obtained with the same data sampling correctly identifies the major areas of lightning occurrence.

3. In cases where the LEP detection site or its conjugate point was within 1000 km of operating VLF receivers at Siple Station or Palmer in Antarctica, a ducted whistler and caus-

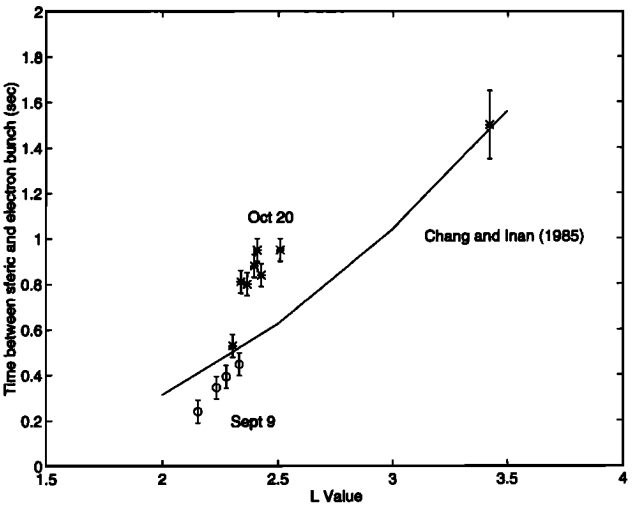

Figure 18. Time delay between sferic and the arrival of the maximum of the precipitating electron burst. Time delays on different days will differ since plasmaspheric electron concentrations are not the same.

ative sferic could usually be identified. This finding suggests that LEP events are produced primarily by the ducted component of whistlers.

4. Assuming that the ducted component of lightning-produced whistlers is responsible for LEP, the transverse dimensions of ducts can be inferred from the pattern of precipitating electrons observed by SEEP at low altitude. The electron train of an LEP persists for 2–3 s during which time the SEEP satellite moves ~16–24 km in latitude. In the 25 cases of strong LEP studied to date, the first pulse (easily identified by its pitch angle distribution peaked at 90°) was always observed. Also, no cases were found where the train terminated abruptly as would be expected if the satellite left the magnetic projection of the duct during the precipitation event. It is thus apparent that the latitude extent of ducts involved in LEP is much greater than 20 km. Evidence of larger duct sizes is found in cases where several LEP events occurred in rapid succession, showing that the satellite was on the field lines passing through a duct for an extended period of time. Figures 4, 5, and 6 indicate that these ducts extended at least 320, 185, and 80 km in latitude. Figures 4, 5, and 6 are in agreement with duct dimensions of 150–300 km recently inferred by *Lev-Tov and Inan* [1996], who compared VLF transmission anomalies observed on closely spaced paths through the precipitation region.

5. Accurate estimates of the loss rates of trapped electrons due to pitch angle diffusion driven by ducted whistler waves from lightning requires a knowledge of the ducted whistler occurrence rates, the distribution of electron deflections by the waves, the number of ducts excited in each event, and the transverse dimensions of the average duct. The electron deflections were measured directly by the SEEP instruments for electrons near the edge of the loss cone. Using measurements of whistler rates observed in Antarctica and assuming the average number of ducts is 10, the electron lifetime at $2 < L < 3.5$ for ≈150 keV electrons is ≈360 days for an average duct radius of 25 km and 22 days for a duct radius of 100 km. Since the footprint dimensions of LEP are >25 km, it appears that ducted whistlers may be an important loss mechanism for electrons in the slot region. If the nonducted component of whistler waves is also effective in precipitating electrons, these lifetimes will be further reduced.

Acknowledgments. We thank R. G. Joiner of the Office of Naval Research (ONR) for the management and coordination of the various elements of the SEEP program. We additionally appreciate help and support from our colleagues at Stanford University, especially D. L. Carpenter, R. A. Helliwell, and V. S. Sonwalkar. The SEEP project at Lockheed Martin was sponsored by ONR under contract N00014-79-C-0824 and at Stanford University under contract N00014-82-K-0489. This recent analysis work at Taylor University, Lockheed Martin, and Stanford University was sponsored by NSF under grant ATM-9513241. A portion of the data analysis was supported by the Lockheed Martin Independent Research Program.

The Editor thanks J. Lichtenberger and another referee for their assistance in evaluating this paper.

References

Angerami, J. J., Whistler duct properties deduced from VLF observations made with the OGO 3 satellite near the magnetic equator, *J. Geophys. Res.*, *75*, 6115, 1970.

Bernhardt, P. A., and C. G. Park, Protonospheric-ionospheric modeling of VLF ducts, *J. Geophys. Res.*, *82*, 5222, 1977.

Burgess, W. C., and U. S. Inan, The role of ducted whistlers in the precipitation loss and equilibrium flux of radiation belt electrons, *J. Geophys. Res.*, *98*, 15,643, 1993.

Calvert, W., H. D. Voss, and T. C. Sanders, A satellite imager for atmospheric x-rays, *IEEE Trans. Nucl. Sci.*, *NS-32*, 122, 1985.

Carpenter, D. L., Recent research on the magnetospheric plasmapause, *Radio Sci.*, *3*, 719, 1968.

Carpenter, D. L., and R. R. Anderson. An ISEE/whistler model of equatorial electron density in the magnetosphere, *J. Geophys. Res.*, *97*, 1097, 1992.

Carpenter, D. L., and D. M. Sulic, Ducted whistler propagation outside the plasmasphere, *J. Geophys. Res.*, *93*, 9731, 1988.

Carpenter, D. L., U. S. Inan, M. L. Trimpi, R. A. Helliwell, and J. P. Katsufrakis, Perturbations of subionospheric LF and MF signals due to whistler-induced electron precipitation bursts, *J. Geophys. Res.*, *89*, 9857, 1984.

Carpenter, G. B., and L. Colin, On a remarkable correlation between whistler-mode propagation and high frequency northscatter, *J. Geophys. Res.*, *65*, 5649, 1963.

Chang, H. C., and U. S. Inan, Lightning-induced energetic electron precipitation from the magnetosphere, *J. Geophys. Res.*, *90*, 4531, 1985.

Cornwall, J. M., Scattering of energetic trapped electrons by very low frequency waves, *J. Geophys. Res.*, *69*, 1251, 1964.

Dungey, J. W., Loss of Van Allen electrons due to whistlers, *Planet. Space Sci.*, *11*, 591, 1963.

Faith, J., S. Kuo, and J. Huang, Electron precipitation caused by chaotic motion in the magnetosphere due to large-amplitude whistler waves, *J. Geophys. Res.*, *102*, 2233, 1997.

Goldberg, R. J., S. A. Curtis, and J. R. Barcus, Detailed spectral structure of magnetospheric electron bursts precipitated by lightning, *J. Geophys. Res.*, *92*, 2505, 1987.

Helliwell, R. A., J. P. Katsufrakis, and M. L. Trimpi, Whistler-Induced amplitude perturbation in VLF propagation, *J. Geophys. Res.*, *78*, 4679, 1973.

Ikeda, M., K. Tsuruda, and S. Machida, Exit areas of VLF waves inferred from multistation measurements at Roberval, Canada, *J. Geomagn. Geoelectr.*, *40*, 227, 1988.

Imhof, W. L., H. D. Voss, M. Walt, E. E. Gaines, J. Mobilia, D. W. Datlowe, and J. B. Reagan, Slot region electron precipitation by lightning, VLF chorus, and plasmaspheric hiss, *J. Geophys. Res.*, *91*, 8883, 1986.

Imhof, W. L., H. D. Voss, J. Mobilia, M. Walt, U. S. Inan, and D. L. Carpenter, Characteristics of short-duration electron precipitation bursts and their relationship with VLF wave activity, *J. Geophys. Res.*, *94*, 10,079, 1989.

Inan, U. S., Gyroresonant pitch angle scattering by coherent and incoherent whistler mode waves in the magnetosphere, *J. Geophys. Res.*, *92*, 127, 1987.

Inan, U. S., and T. F. Bell, The plasmapause as a VLF wave guide, *J. Geophys. Res.*, *82*, 2819, 1977.

Inan, U. S., and D. L. Carpenter, On the correlation of whistlers and associated subionospheric VLF/LF perturbations, *J. Geophys. Res.*, *91*, 3106, 1986.

Inan, U. S., T. F. Bell, and R. A. Helliwell, Nonlinear pitch angle scattering of energetic electrons by coherent VLF waves in the magnetosphere, *J. Geophys. Res.*, *83*, 3235, 1978.

Inan, U. S., T. G. Wolf, and D. L. Carpenter, Geographic distribution of lightning-induced electron precipitation observed as VLF/LF perturbation events, *J. Geophys. Res.*, *93*, 9841, 1988.

Inan, U. S., M. Walt, H. D. Voss, and W. L. Imhof, Energy spectra and pitch angle distributions of lightning-induced electron precipitation: Analysis of an event observed on the S81-1 (SEEP) satellite, *J. Geophys. Res.*, *94*, 1379, 1989.

Janes, H. G., Refraction of whistler mode waves by large scale gradients in the middle latitude ionosphere, *Ann. Geophys.*, *28*, 301, 1972.

Kennel, C. F., and H. E. Petschek, Limit on stably trapped particle fluxes, *J. Geophys. Res.*, *71*, 1, 1966.

Lev-Tov, S. J., U. S. Inan, A. J. Smith, and M. A Clilverd, Characteristics of localized ionospheric disturbances inferred from VLF measurements at two closely spaced receivers, *J. Geophys. Res.*, *101*, 15,737, 1996.

Lyons, L. R., R. M. Thorne, and C. F. Kennel, Pitch angle diffusion of radiation belt electrons within the plasmasphere, *J. Geophys. Res.*, *77*, 355, 1972.

Maehlum, B., and J. Stadsnes, Scattering and absorption of fast electrons in the upper atmosphere, Phys. Norw., *2*, 111, 1067.

Mobilia, J., H. D. Voss, and W. L. Imhof, Lightning observations from the SEEP/S81-1 satellite (abstract), *EOS Trans. AGU*, *66*, 1001, 1985.

Roberts, C. S., Pitch angle diffusion of electrons in the magnetosphere, *Rev. Geophys.*, *7*, 305, 1969.

Rosenberg, T. J., R. A. Helliwell, and J. P. Katsufrakis, Electron precipitation associated with discrete, very low frequency emissions, *J. Geophys. Res.*, *76*, 8445, 1971.

Rycroft, M. J., Enhanced energetic electron intensities at 100 km altitude and a whistler propagating through the plasmasphere, *Planet. Space Sci.*, *21*, 239, 1973.

Schulz, M., and L. J. Lanzerotti, *Particle Diffusion in the Radiation Belts*, Springer-Verlag, New York, 1974.

Sonwalkar, V. S., U. S. Inan, T. F. Bell, R. A. Helliwell, V. M. Chmyrev, Y. P. Sobolev, O. Y. Ovcharenko, and V. Selegij, Simultaneous observations of VLF ground transmitter signals on the DE-1 and COSMOS 1809 satellites: Detection of a magnetospheric caustic and a duct, *J. Geophys. Res.*, *99*, 17,511, 1994.

Stadsnes, J., and B. Maehlum, Scattering and absorption of fast electrons in the upper atmosphere, *Intern Rep. E-53*, Forsvarets Forskningsinstitutt, NDRE, Kjeller, Norway, 1965.

Strangeways, H. J., and M. J. Rycroft, Trapping of whistler-waves through the side of ducts, *J. Atmos. Terr. Phys.*, *42*, 983, 1980.

Teague, M. J., and J. I. Vette, The use of the inner zone electron model AE-5 and associated computer programs, *Rep. NSSDC 72-11*, Goddard Space Flight Cent., Greenbelt, Md., 1972.

Vampola, A. L., Observations of VLF transmitter-induced depletions of inner zone electrons, *Geophys. Res. Lett.*, *10*, 619, 1983.

Voss, H. D., W. L. Imhof, D. O. Murray, D. A. Simpson, D. P. Caufman, and J. C. Bakke, Low temperature characteristics of solid state detectors for energetic X ray, ion and electron spectrometers, *IEEE Trans. Nucl. Sci.*, *NS-29*, 164, 1982a.

Voss, H. D., J. C. Bakke, and S. N. Roselle, A spacecraft multichannel analyzer for a multidetector solid state detector array, *IEEE Trans. Nucl. Sci.*, *NS-29*, *173*, 1982b.

Voss, H. D., W. L. Imhof, J. Mobilia, E. E. Gaines, M. Walt, U. S. Inan, R. A. Helliwell, D. L. Carpenter, J. P. Katsufrakis, and H. C. Chang, Lightning-induced electron precipitation, *Nature*, *312*, 740, 1984.

W. L. Imhof and J. Mobilia, Lockheed Martin Advanced Technology Center, Palo Alto, CA 94304.

U. S. Inan and M. Walt, STAR Laboratory, Stanford University, Stanford, CA 94305.

H. D. Voss, Department of Physics, Taylor University, Upland, IN 46989.

(Received July 8, 1997; revised September 29, 1997;
accepted September 30, 1997.)